

# Software and Simulation for $Q_{\text{weak}}$

Erin H. Epperson

*Department of Physics, College of William and Mary,  
Williamsburg, VA 23188*

(Dated: April 16, 2004)

## **Abstract**

The drift chamber simulation program GARFIELD was used to perform a variety of simulations relating to the performance of drift-time properties of the Jefferson Lab Hall C proposed Vertical Drift Chamber. Simulations for this drift chamber were used to explore the properties of the Vertical Drift Chamber (VDC) to aid in the initial testing and construction of a new VDC for Hall C to be used for the  $Q_{\text{weak}}$  experiment. This new experiment will provide a more precise measurement of the weak charge of the proton.

# Contents

|   |           |
|---|-----------|
| <b>1. Introduction</b>                                | <b>4</b>  |
| <b>2. The <math>Q_{\text{weak}}</math> Experiment</b> | <b>6</b>  |
| 2.1 Goals of the Experiment .....                     | 6         |
| 2.2 The Physics of $Q_{\text{weak}}$ .....            | 11        |
| <b>3. Drift Chambers</b>                              | <b>14</b> |
| 3.1 Components of a Drift Chamber .....               | 14        |
| 3.2 Physics of a Drift Chamber .....                  | 16        |
| 3.3 A Vertical Drift Chamber .....                    | 20        |
| <b>4. Jefferson Lab Vertical Drift Chamber</b>        | <b>21</b> |
| <b>5. Drift Time Simulations</b>                      | <b>23</b> |
| 5.1 Introduction to GARFIELD.....                     | 23        |
| 5.2 Taming the Beast: Troubleshooting GARFIELD.....   | 24        |
| 5.3 Drift Time Behavior using GARFIELD.....           | 25        |
| 5.4 Conclusion .....                                  | 41        |
| <b>A. GARFIELD Input</b>                              | <b>42</b> |
| A.1 The Cell .....                                    | 42        |
| A.2 Gas Parameters .....                              | 43        |
| A.3 Electric Field .....                              | 44        |
| A.4 Drift Properties .....                            | 46        |
| A.4.1 DRIFT .....                                     | 46        |
| A.4.2 X-T PLOT .....                                  | 48        |
| A.4.3 ARRIVAL .....                                   | 51        |

|                    |           |
|--------------------|-----------|
| A.4.4 SIGNAL ..... | 55        |
| A.4.5 TIMING ..... | 59        |
| <b>B. Tables</b>   | <b>62</b> |
| <b>References</b>  | <b>66</b> |

# Chapter 1

## Introduction

New theories are proposed daily to explain phenomena in the world of particle physics. The Thomas Jefferson National Accelerator Facility (Jefferson Lab) contains three experiment halls dedicated to research in Nuclear Physics using electrons as projectiles. Starting in a few years time, Hall C of Jefferson Lab will be dedicated to the experiment known as  $Q_{\text{weak}}$  [3]. A group of physicists working at Jefferson Lab has proposed an experiment to measure the weak mixing angle of the proton via parity-violating electron scattering on the proton at very low  $Q^2$ .

An important component of the experiment will be conducted using Vertical Drift Chambers (See Chapter 3). The drift chamber measures the drift time of an electron to a wire to determine the trajectory of the original track produced by an incoming particle (in this case, the elastically scattered electrons).

Simulations in this thesis are dedicated to exploring the geometry of the proposed drift chamber for the experiment. GARFIELD, a drift chamber simulation program designed by Rob Veenhof at CERN, allows one to simulate various aspects of the physics in the drift chamber and output information including track, electric field,  $x(t)$  relations, arrival-time distributions, and drift time data [1]. Interfaced with the program MAGBOLTZ, written by Steve Biagi, GARFIELD can calculate gas properties in mixtures of various commonly used gases. GARFIELD is constantly under revision. Test runs in the initial stage of this research were conducted using version 7.04. Halfway

into the stages of my research, Klaus Grimm of William and Mary compiled a newer version [2] (Version 8.10-1a) which I used for the data found in the body of this paper. Input files used for these simulations are found in Appendix A.

Chapter Two of this thesis explains in greater detail the goals of  $Q_{\text{weak}}$ . Chapter Three explains the theory of vertical drift chambers. Chapter Four details the parameters of the proposed Hall C Vertical Drift Chamber including specifics such as drift time distribution. Chapter Five covers the details of GARFIELD, including how it operates, how calculations are performed and suggestions for troubleshooting GARFIELD. It also includes the results of this research and some possible implications for  $Q_{\text{weak}}$ .

## Chapter 2

### The $Q_{\text{weak}}$ Experiment

#### 2.1 Goals of the Experiment

Jefferson Lab has proposed and received preliminary funding for trial runs of the  $Q_{\text{weak}}$  experiment.  $Q_{\text{weak}}$  proposes the first precision measurement of the weak charge of the proton by measuring the parity-violating asymmetry in electron-proton ( $ep$ ) elastic scattering at low momentum transfer. The weak mixing angle ( $\sin^2\theta_w$ ) is related to the relative effects of the Electromagnetic forces compared to the effects of the weak force for a given momentum transfer. This angle varies with momentum transfer as shown in Figure 2.1. Determining this weak mixing angle requires a set of precision measurements at a variety of energy scales [3].

The  $Q_{\text{weak}}$  experiment uniquely combines a high beam current, low momentum transfer ( $Q^2 \sim 0.003 \text{ GeV}/c^2$ ), and a dedicated apparatus. The apparatus will be designed uniquely for this experiment unlike previous measurements of the weak charge. A new level of precision allows Standard Model predictions to be either confirmed or rejected. If results differ significantly from the Standard Model prediction, it could lead the way for a new understanding of physics. Elastic scattering of the electron and proton at a fixed  $Q^2 = 0.003 \text{ (GeV}/c^2)$  will allow the researchers to measure the weak charge [4].

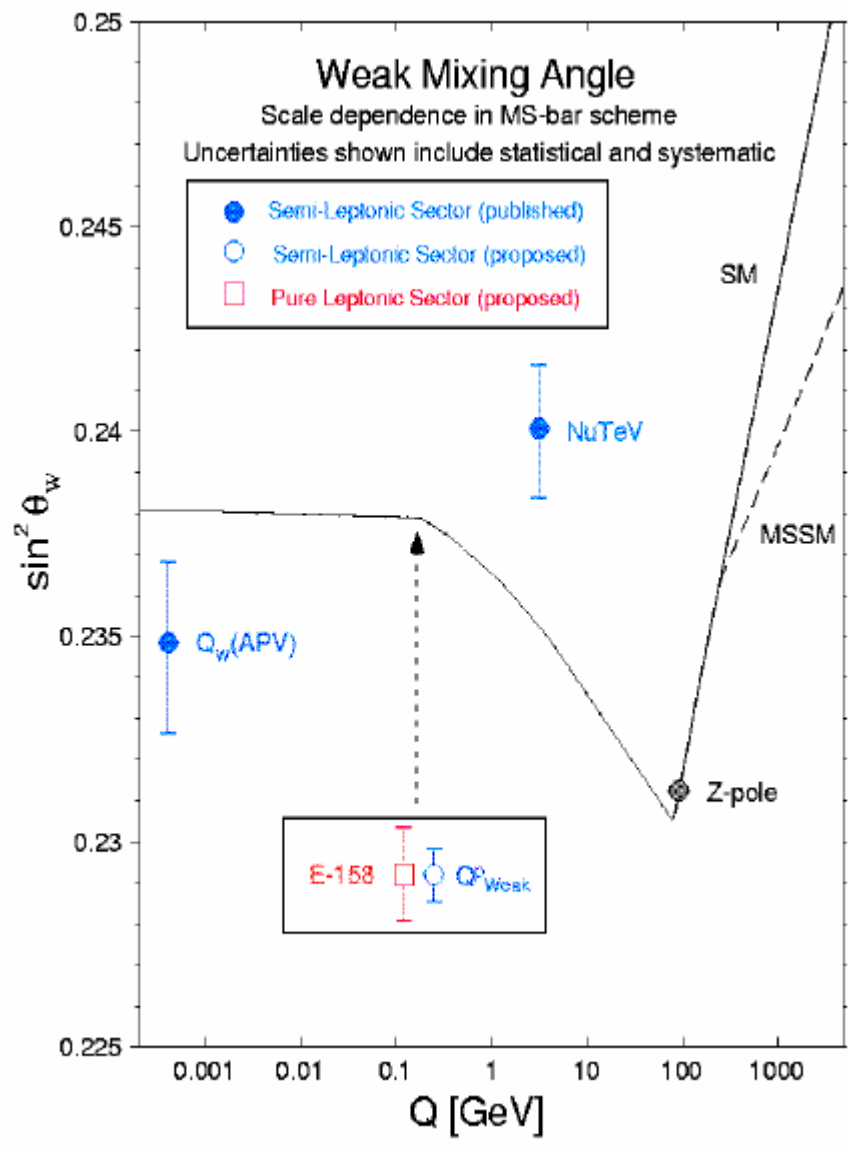


Figure 2.1 - This was taken from the  $Q_{\text{weak}}$  proposal [4]. The figure depicts the measured data points and theoretical weak mixing angle ( $\sin^2 \theta_w$ ) for all values of  $Q^2$ . The region  $Q_{\text{weak}}$  is concerned with is within what is predicted to be a relatively constant area ( $Q < 0.1$ ).

Jefferson Lab will use a toroidal magnet (Figures 2.3 & 2.4) to focus scattered electrons onto a set of eight fused silica Cerenkov detectors. The Cerenkov detectors (Figure 2.2) act as a counter. The detectors give a pulse of light when hit, but where on the detector the electron hit is unknown. The purpose of the drift chambers that are the focus of this thesis is to reconstruct the track and hence the position of the electron when it hits the detector. In the main measurement the scattered electron rate will prevent the use of tracking chambers to reconstruct the trajectory. To ensure that the Cerenkov detectors are measuring elastically-scattered electrons (and to determine their  $Q^2$ ), in a set of supplementary measurements the beam current will be reduced several orders of magnitude, and a set of three regions of tracking chambers (CD1, DC2, and the VDC) will be installed.

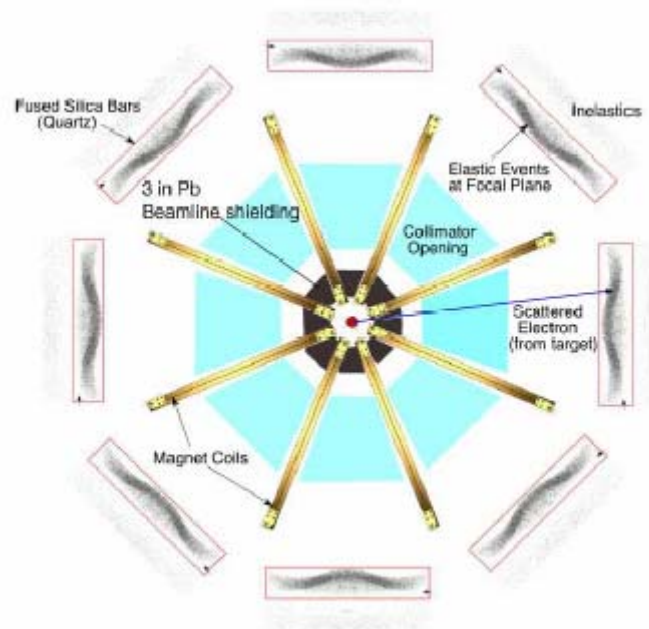


Figure 2.2 – Cerenkov Detectors. Each time an electron hits a detector, a dot is added to the spot hit to visually represent the distribution of electrons. [3]

The drift chamber simulated for this thesis only determines the electron's trajectory as it exits the magnet and heads to the Cerenkov detector. Within the apparatus (Figure 2.4), two other drift chambers (DC1 and DC2) will determine the scattering angle  $\theta$ . The combination of the track momentum (determined by the magnetic field and the trajectory seen by the VDC) and  $\theta$  give us  $Q^2$  and separates elastic from inelastic events. The events due to inelastic scattering are then ignored and only the elastically scattered electrons are considered for study. The physics of determining the weak charge via this information will be discussed in the next section.

Jefferson Lab will conduct a 2200 hour measurement of the parity violating asymmetry in electron-proton scattering involves the elastic scattering of electrons on a 35 cm liquid Hydrogen target. This should determine the proton's weak charge within a 4% combined statistical and systematic margin or error. This experiment is also unique in that it will be the first precision Standard Model test to be performed at Jefferson Lab [4].

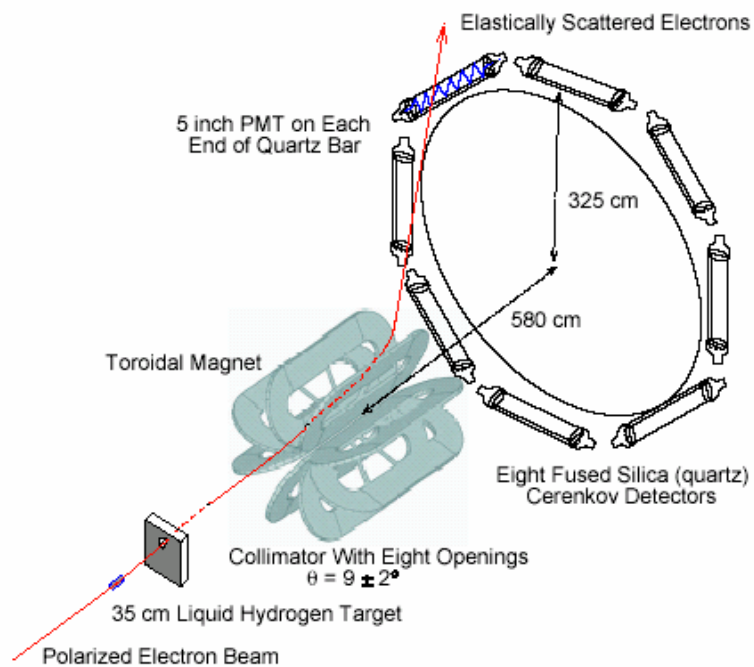


Figure 2.3 – Overview of the Qweak apparatus. The VDC will be located between the magnet and the Cherenkov detectors. [3]

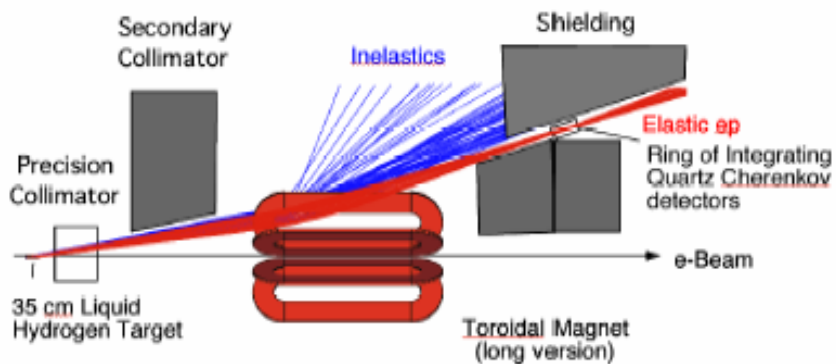


Figure 2.4 - A rough depiction of the apparatus to be constructed for  $Q_{\text{weak}}$  [7].

## 2.2 The Physics of $Q_{\text{weak}}$

The weak charge of the proton can be measured via parity-violating statistics in scattering electrons against protons.  $A_{\text{LR}}$  (Equation 1) is defined as the asymmetry in the measurement of the cross section difference between elastic scattering of left-handed and right-handed longitudinally polarized electrons. Referring back to Figure 2.2, the number of electrons with spin along the direction of motion (right-handed,  $\sigma_+$ ) that hit the Cerenkov detector does not equal the number of electrons with spin opposite their direction of motion (left-handed,  $\sigma_-$ ). This asymmetry ( $A_{\text{LR}}$ ) is measured by the difference of those two values divided by the total number of hits.

$$A = \frac{\sigma_+ - \sigma_-}{\sigma_+ + \sigma_-} \quad (1)$$

This asymmetry is also proportionally related to the weak charge of the proton and the momentum transfer as given below.

$$A_{\text{LR}} \propto Q^2 Q_{\text{weak}}^p + A_s Q^4 \quad (2)$$

$A_s$  is the coefficient related to strong interaction effects. At low  $Q^2$ , the first term dominates such that the asymmetry is approximately equal to the momentum transfer,  $Q^2$  (which in the  $Q_{\text{weak}}$  experiment is precisely determined), multiplied by the weak charge of the proton ( $Q_{\text{weak}}^p$ ). The measured weak charge of the proton gives us the weak mixing angle for low momentum transfer (Equation 3).

$$Q_{\text{weak}} = Q_w^p = 1 - 4\sin^2\theta_w \quad (3)$$

Comparing this experimental value to the Standard Model predictions (Figure 2.1) allows the Standard Model to either be confirmed or else lead the way to new physics beyond the Standard Model.

At high  $Q^2$  values, the weak mixing angle is known through precise measurements. At low  $Q^2$ , atomic parity violations have given us a range of possibilities for the weak mixing angle. Figure 2.2 (taken from the  $Q_{\text{weak}}$  proposal) shows the experimental values of  $Q^2$ . Through multiple precision measurements at low  $Q^2$ , extraction of the weak mixing angle  $\sin^2\theta_w$  is attainable [4]. The theoretically expected variation in  $\sin^2\theta_w$  seen in Figure 2.2 is due to high-order processes (loops, etc.) involving all the particles in the Standard Model.

Hints of deviation from the Standard Model can be found in experiments measuring the weak charge of Cesium, but the universality of these results are inconclusive as they involve a certain uncertainty because of unknown characteristics of the atomic structure of Cesium. By comparison, the  $Q_{\text{weak}}$  experiment seeks to measure the parity-violating asymmetry, which does not require the uncertain theoretical atomic physics the Cesium experiment did. The Cesium experiment led to findings significantly below the predictions of the Standard Model which could not be filtered further due to uncertainty in the physics of the atomic structure of the Cesium atom [4].

The Standard Model predicts the behavior of  $Q_w^p$  based on measurements at low energies. Some theorists believe there are several reasons to reevaluate the Standard Model theory. The properties of a large number of parameters including masses, mixing angles, and couplings, are not a natural result of the theory, but rather have to be worked in to fit. In addition, The Standard Model fails to explain discrete phenomena such as

why parity violation occurs. Rather it incorporates these phenomena into the framework of the theory without searching for deeper explanations. The weak charge of the proton is a property that has never been precisely measured before. For protons, more of the structure is known and therefore uncertainties are minimalized for low  $Q^2$ , hence the asymmetry ( $A_{LR}$ ) is more confidently determined (Equations 2 and 3). Simulations of the drift chamber help construct the track of the electron and hence determine the kinematics of the data ( $Q^2$ ). Combined with the other two drift chambers which tell us which events to consider (elastic or inelastic scattering), the drift chamber closest to the Cerenkov detectors allows us to determine the position and number of hits on the detector and hence the  $Q^2$ . Simulations of the drift chamber done in this thesis aim to provide an understanding of the reconstruction of the track via the drift time as well as an understanding of the correctional values in the position of the electron on the detector as addressed in Chapter 5 of this thesis.

## Chapter 3

### Drift Chambers

#### 3.1 Components of a Drift Chamber

A drift chamber is composed of a gas-filled volume with an applied Electric Field. A drift chamber is used to measure an electron's drift time [5] to obtain measurements about its initial track (Figures 3.1, 3.2). A simple drift chamber contains a single cell with an electric field and a proportional counter to measure the time between ionization and arrival of the electron, to be described in the next section. The gas chosen for the medium affects the velocity and ionization rate of electrons; hence, a unique gas mixture should be chosen to obtain the most detectable results in experimentation. Avalanche multiplication (to be explained in the next section) occurs at lower fields in noble gases than in more complex gases. Since Argon has a high specific ionization and is not as expensive as some of the other noble gases (such as xenon or krypton), it is often used in drift chambers [5]. The gas mixture assumed for the present simulations has been argon-ethane (50/50).

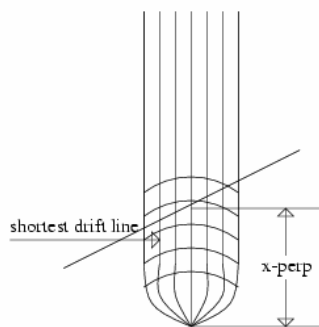


Figure 3.1 – Electric Field lines and isochrones for a wire in a wire chamber [6]. The x-perpendicular distance is the desired measured distance. The drift time gives us the distance of the curved line.

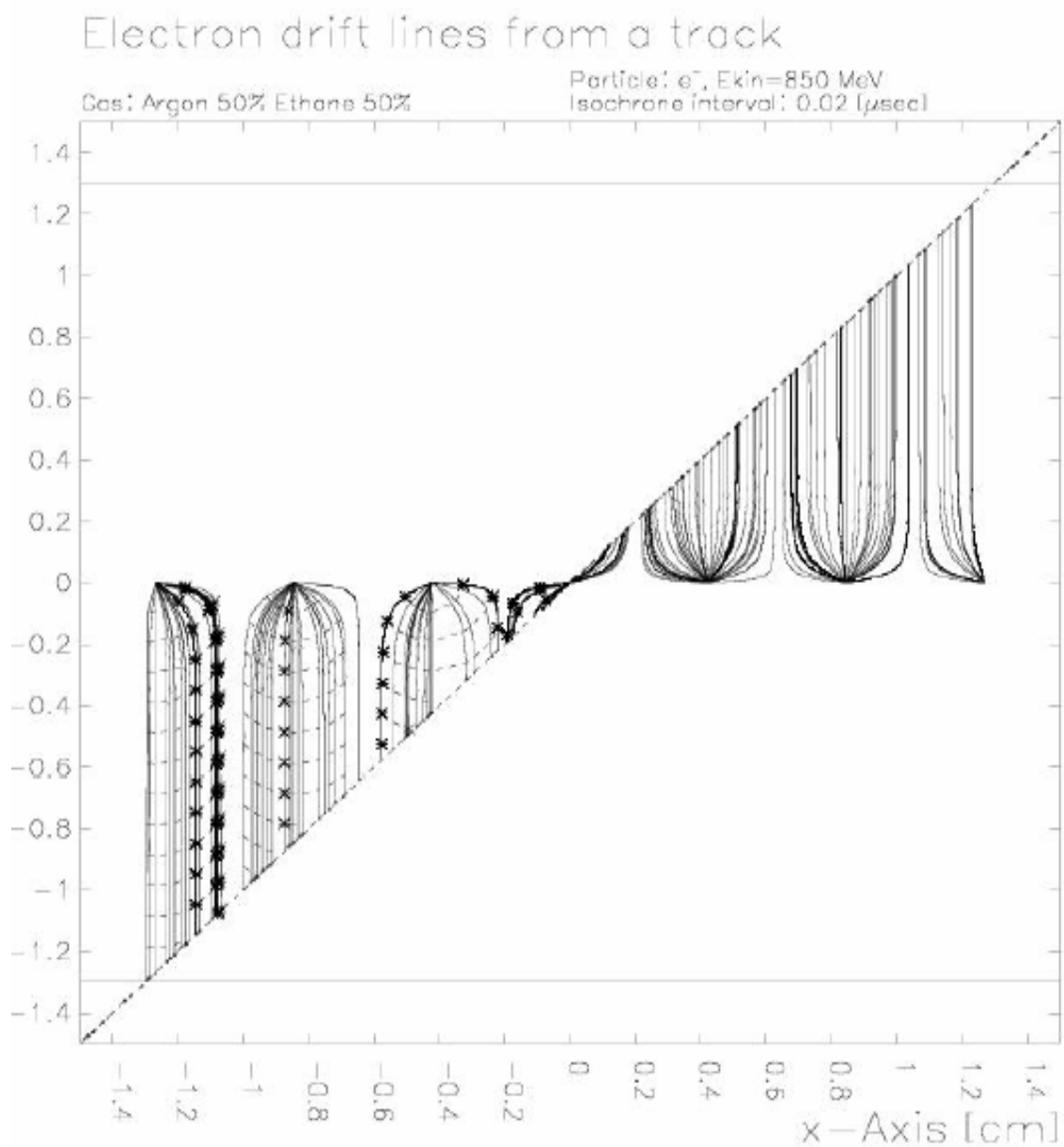


Figure 3.2 – The track of a sample electron. The initial particle continues along the given track and scattered electrons drift to the wires in the pattern given by the curved lines to the points representing the charged wires. The planes ( $\pm 1.3$  cm) are charged to a  $-V$  voltage and the wires by contrast are held at ground.

### 3.2 Physics of a Drift Chamber

When a charged particle enters the chamber, it collides with gas molecules. The effect on the gas molecules is dependent on the velocity of electron as well as its mass and charge, given by the Bethe-Bloch formula [5].

$$\frac{dE}{dX} = -K \frac{Z}{A} \frac{\rho}{\beta^2} \left\{ \ln \frac{2mc^2\beta^2 E_M}{I^2(1-\beta^2)} - 2\beta^2 \right\} \quad (4)$$

If the charged particle is energetic enough, in transferring some of its energy to a molecule, an electron-ion pair is produced. The voltage of the planes relative to the uncharged wires causes the ion to drift to the planes and the electron to drift to the wires. Closer to the wire, the electron from the initial electron-ion pair accelerates, gaining more energy. It can collide with another gas molecule and create another electron-ion pair. Since this pair is even closer to the wire, it gains even more energy through acceleration to the wire and collides with another molecule. Meanwhile the initial electron is colliding with other molecules and through continuous collision and acceleration close to the wires what is known as an “avalanche affect” occurs [5]. Instead of one electron accelerating towards the wire we now have many. The total time it takes one of these electrons to “drift” to the closest wire is known as the drift time ( $t_d$ ). The velocity at which the electron drifts to the wire is called the drift velocity ( $v_d$ ). Since the acceleration due the wire is stronger the closer the electron is to the wire, the drift velocity is relatively constant far away from the wires (along the original track), but increases and becomes approximately quadratic within the “avalanche region,” due to the increased electric field in that region (Figure 3.3). For the region of constant drift velocity, the coordinate of the track with respect to the wire is the linear relation given in Equation 5, where  $t_1-t_0$

represents the  $\Delta t$  or time passed before arrival at the given x-value. From this equation,  $t_1$  is the drift time measured and  $t_0$  is the drift time from that given x-value to the wire.

$$x = (t_1 - t_0) v_d. \quad (5)$$

Since for the avalanche region, the drift time increases as the distance from the wire decreases, the  $x(t)$  relation for the avalanche region resembles a quadratic, which will be discussed further in Chapter 5 of this thesis. Figures 3.3, 3.5 illustrates the difference in drift velocities for linear and avalanche regions for the first electron.

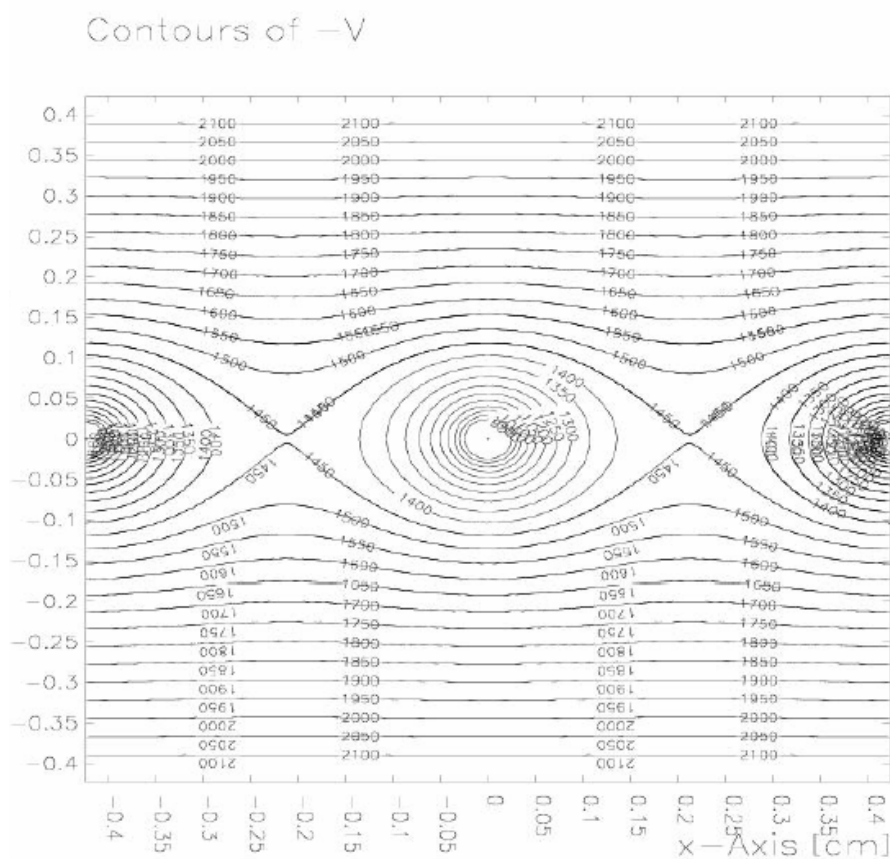


Figure 3.3 - The equipotentials at the location of the wires, clearly demonstrating the avalanche effect of the electrons near the charged wires. The close concentric circles around the wires depicted define the area where the avalanche effect will occur. Figure 3.5 shows the consequences of this effect.

A plot of the  $X(t)$  relation for the drift time and measured position (Figure 3.4) demonstrates the differences in inverse of velocity between the constant velocity away from the wires and the velocity within the avalanche region. The  $X(t)$  plot gives the horizontal distance the electron traveled to the wire from the track.

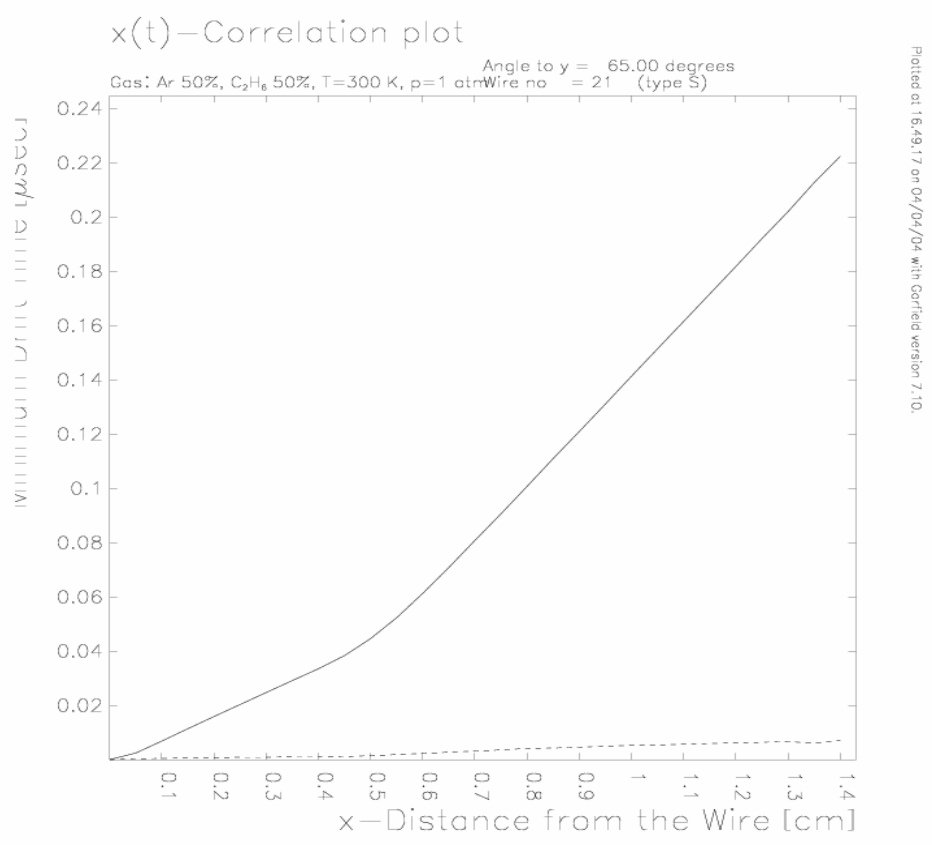


Figure 3.4 – An  $x(t)$  plot for the first electron to hit a given wire. From the plot one can see that the avalanche region starts around 0.4 cm from the wire in this case.

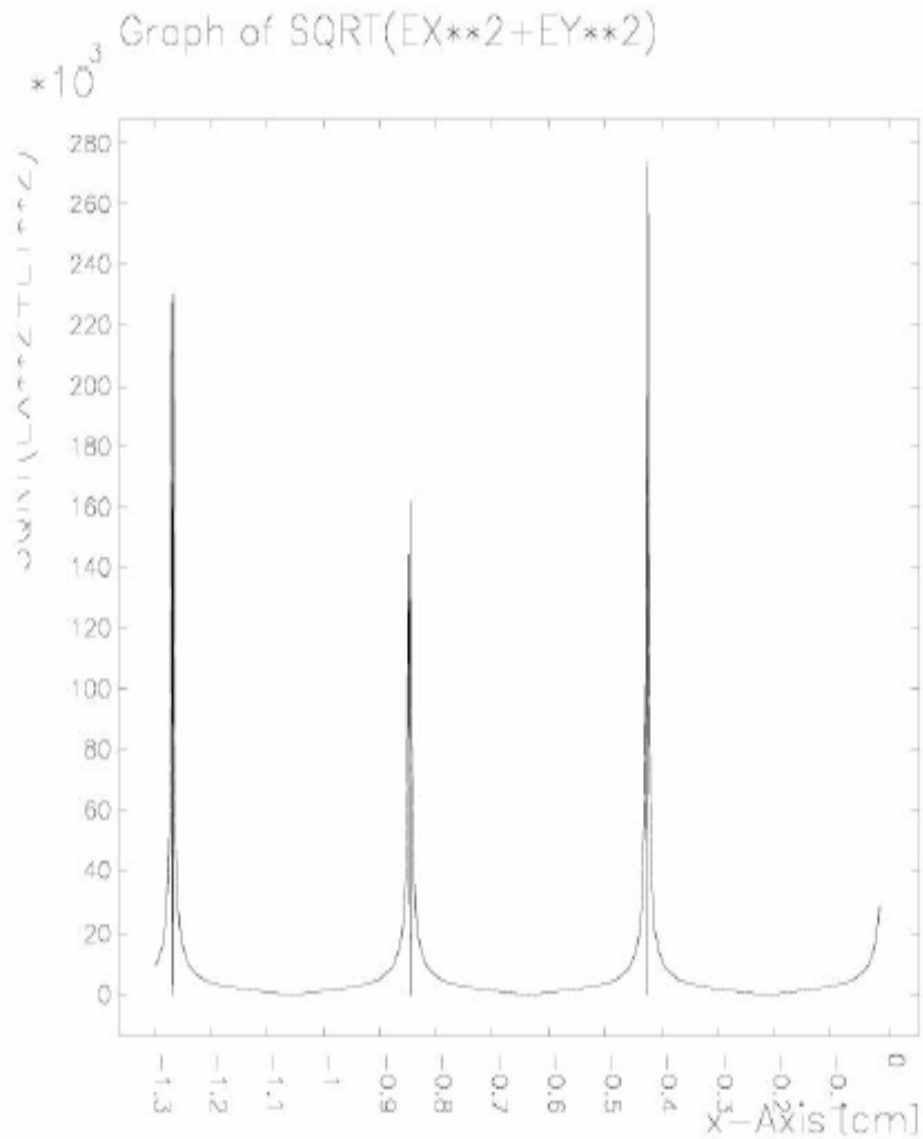


Figure 3.5.  $-(E_x^2 + E_y^2)^{1/2}$  vs. x (location along the sense wire plane). Illustrates the avalanche effect near the wires. Looking at the peaks from a position above the peaks gives the view shown in Figure 3.3. The peaks represent the electric field at each wire. The acceleration of electrons close to the wires creates a dramatic increase in the electric field immediately close to the wire which drops off sharply away from the wire.

### 3.3 A Vertical Drift Chamber

A Vertical Drift chamber differs from an ordinary single-cell drift chamber in many ways. A Vertical Drift Chamber (VDC) consists of multiple planes of gas-filled volumes. The wires are arranged in parallel rows along the horizontal axis. The reason it is called a “Vertical” drift chamber is because the configuration of the electric field causes the electron to drift vertically to the wires (Figure 3.6). By comparison, a Horizontal Drift Chamber is configured so that the shortest drift distance is horizontally to the wire [7]. The reason the plots of the drift time in this thesis are  $X(t)$  plots and not  $Y(t)$  plots is because GARFIELD only calculates steps in the X-direction. As a result we flipped the layout of the chamber  $90^\circ$  in the simulation (See Appendix A for the input code). More information about VDCs can be found in the following Chapter about the Jefferson Lab Vertical Drift Chambers.

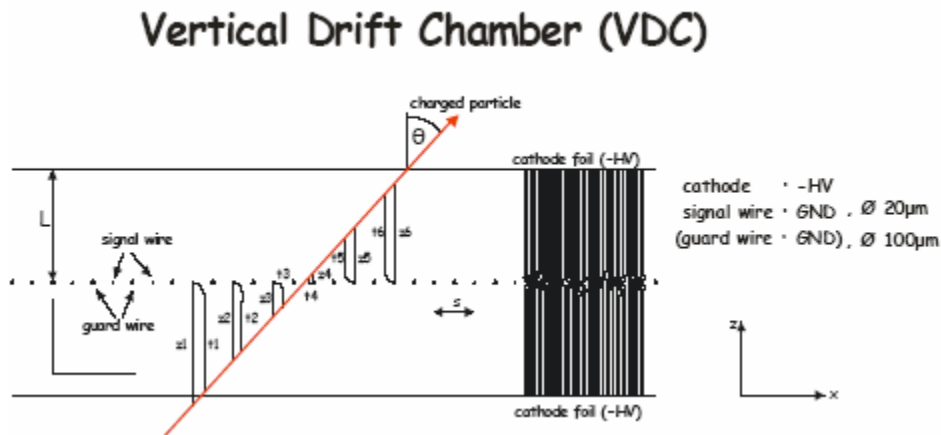


Figure 3.6 - VDC schematic for  $Q_{\text{weak}}$  [7]

## Chapter 4

### Jefferson Lab Vertical Drift Chamber

As mentioned previously, a VDC (Figure 3.6) is a drift chamber where the shortest distance to the wire is in the vertical direction. In Chapter 2, it was explained that there are several drift chambers in the apparatus designed for the  $Q_{\text{weak}}$  experiment. The other two drift chambers help determine whether or not an event is the result of an elastic or inelastic collision. Another added benefit of the other detectors is that they provide a more precise determination of the track. Because of the curvature of the drift of the electron to the wire, there is a certain error involved in the measurement of the track of the initial electron. The measurement of the track in one drift chamber yields a margin of error of about  $1^\circ$ . By comparing the point where the electron started in one drift chamber to the point where the electron left the previous chamber, one can fine-tune the precision to within  $\sim 1\text{-}3$  mrad [3].

Each plane in the Jefferson Lab VDC will have two sets of wires that cross each other at a  $45^\circ$  angle along the horizontal plane (Figure 4.1) [7]. The wires are also oriented at a  $45^\circ$  angle to the plane itself. This serves to prevent the sagging of wires. If the wires are too long, they sag and the force needed to keep them taut would cause them to break. Since the alignment of the wires determine the precision of the measurements, orienting them at  $45^\circ$  to the plane serves to eliminate this problem. More importantly, it aids in resolving ambiguities in reconstruction of the electron's trajectory since the precision given by the taut wires aids in the reconstruction of the angle via the comparison of two points in two different drift chambers mentioned previously.

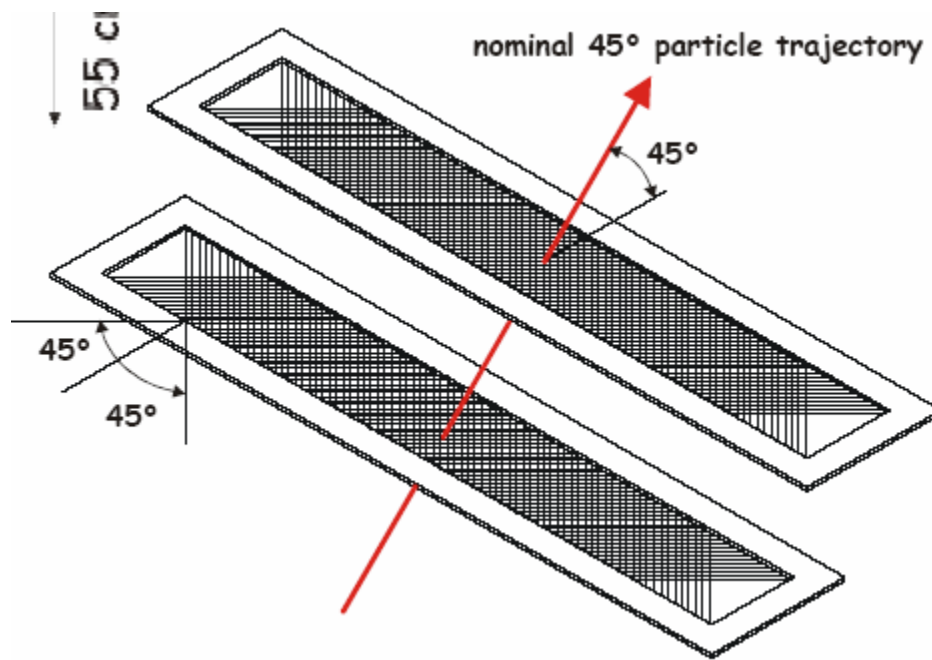


Figure 4.1 – Track of electron through planes in the Vertical Drift Chamber to be used for  $Q_{\text{weak}}$ . [7]

## Chapter 5

# Drift Time Calibration with Garfield

### 5.1 Introduction to Garfield

For this project I used Garfield, a drift-chamber simulation program designed by Rob Veenhof. With the aid of Garfield I was able to simulate two and three-dimensional drift chambers designed to be replicas of the drift chamber to be built in Hall C of Jefferson Lab. I used Garfield to calculate arrival time distributions, drift time tables, field maps and  $x(t)$  relations. The version of Garfield I used in the initial stages of my work was compiled from version 7.04. Halfway into the stages of my research, Klaus Grimm compiled a newer version (Version 8.10-1a) [2] which I used for all further stages of simulation. The older version of Garfield was used mostly in the troubleshooting and exploratory stages of my research in which I was attempting to learn how Garfield operates. Most of the later data, including drift time tables and the  $y$  - correction information was performed on the newer version.

Garfield simulates the properties of the drift chamber indicated in the input file. The user also inputs track information (angle or start and end points) which allows Garfield to simulate drift times of the avalanche particle to the nearest wire and then calculate the particle's original position and velocity. The versions I used allow for two-dimensional simulation of the chamber as well as two-dimensional plots of drift properties and avalanche properties of the particles [1].

To allow others to better understand how to work with Garfield I decided to include a troubleshooting section.

## 5.2 Taming the Beast: Troubleshooting Garfield

In the initial stages of my work, I encountered many glitches, both technological and otherwise. I found that version 5.27 was the earliest user's guide readily available in hardcopy. Though the CERN website had a more updated version of the guide (7.04), the explanations of various input commands were vague at best and incoherent at worst. As a result I have added comments to a majority of the input files included in Appendix A to allow others who may rely on this research to more readily understand the recent versions of Garfield. Similarly, the comments, I hope, allow others the luxury of learning from my experience in dealing with Garfield.

I began my introit into Garfield with a variety of tools and resources. With the version 5.27 guide [9] in one hand, Risa Wechsler's undergraduate thesis [6] in another, and the CERN website [10] on the screen, I attempted to recreate the graphs included in Risa's thesis. By modifying her input files to more closely match the ambiguous examples on the CERN website I was able to recreate graphs that closely resembled the ones in her thesis. There were many minute differences between the input examples from Risa's thesis which used version 5.18 and the final result. Fortunately, the source code for Garfield includes a help section so when Garfield is recompiled, a help interface similar to the interface found on the CERN website [10] is created. The sources for Garfield and the help pages created for Dr. Grimm's compilation can be found on the Jefferson Lab website [2].

### 5.3 Drift Time Behavior using GARFIELD

The table below is created from the data output of the X-T function. The input code is listed in section 4.2 of Appendix A. Using eleven angles ranging from 45° to 65° with a step of 0.05 cm Garfield generated drift times for the first electron along the track to wire 21. For all of the data points, plots of both a linear fit and a quadratic fit were created through Microsoft Excel. The linear section was defined as all points occurring after 0.4 cm. The cutoff was determined by a combination of a plot of arrival time for one electron (Figure 5.2) and comparison with X(t) plots both generated by Excel and by Garfield (Figures 3,4).

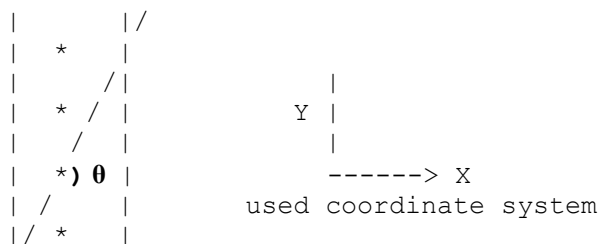


Figure 5.1 Shows the orientation of the drift chamber used for these simulations. GARFIELD only allows for step size in the x-direction, so to enable easier calculations, all simulations for the VDC are done oriented 90° as shown above.  $\theta$  is defined as the angle between the track and the x-axis (starting from the track and moving down to the axis).

Table 1 - Slopes of linear fits to X(t) plots for various track angles ( $\theta$ )

| $\theta$ | Full linear fit | Linear section |
|----------|-----------------|----------------|
| 45       | 0.1883          | 0.1979         |
| 47       | 0.1870          | 0.1988         |
| 49       | 0.1856          | 0.1991         |
| 51       | 0.1836          | 0.1981         |
| 53       | 0.1815          | 0.1980         |
| 55       | 0.1794          | 0.1983         |
| 57       | 0.1763          | 0.1973         |
| 59       | 0.1732          | 0.1973         |
| 61       | 0.1691          | 0.1964         |
| 63       | 0.1646          | 0.1955         |
| 65       | 0.1587          | 0.1935         |

This data represents the comparison of the angle and the slope of the linear fit of the X-T PLOT including the avalanche region. The second slope column refers to the slope of the linear fit to the linear region (data from 0.5 cm and further from the wire so as to not include the avalanche region). The decision to start the linear region at 0.5 cm was determined primarily by the behavior of the plots around the area of 0.3 cm to 0.4 cm. Comparing the linear plots made including or excluding those points led to the conclusion that the linear region is best described in the plots as extending to 0.5 cm from the wire.

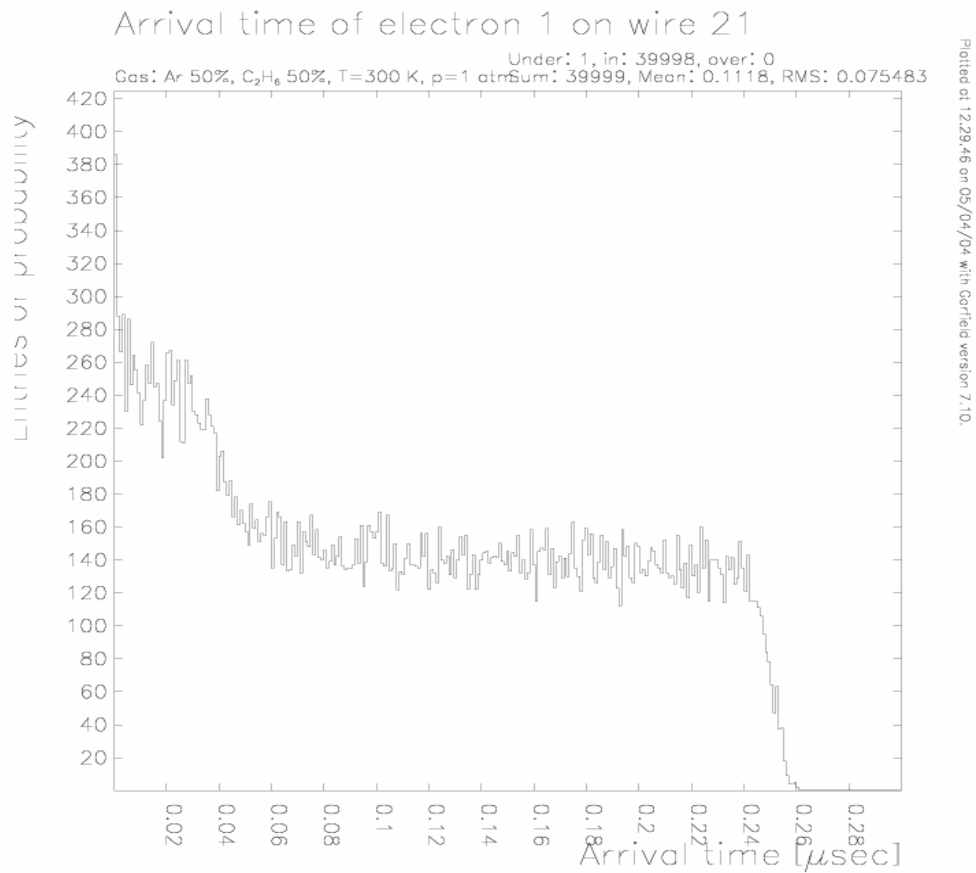
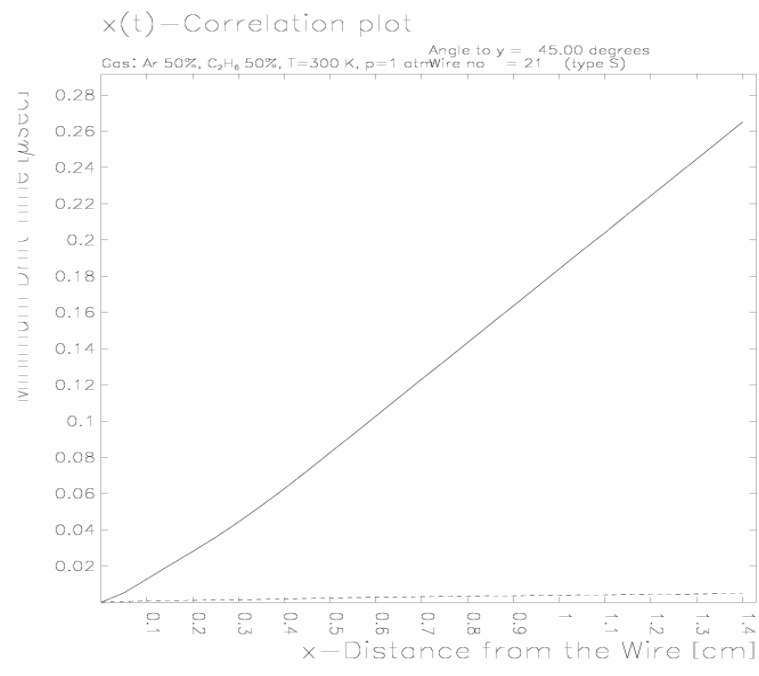
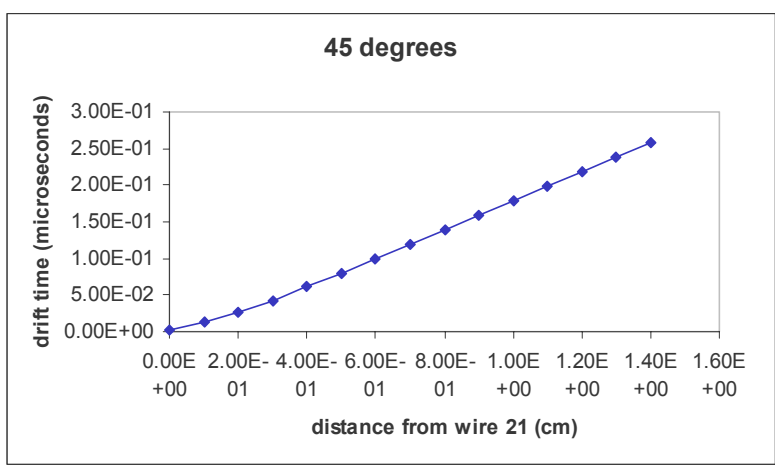


Figure 5.2 - Shows the overall arrival time distribution for the first electron on a wire for all measured angles ( $45^{\circ}$ - $65^{\circ}$  in  $2^{\circ}$  increments). From this, the avalanche region is seen clearly for  $t \approx 0.04 \mu\text{s}$ .



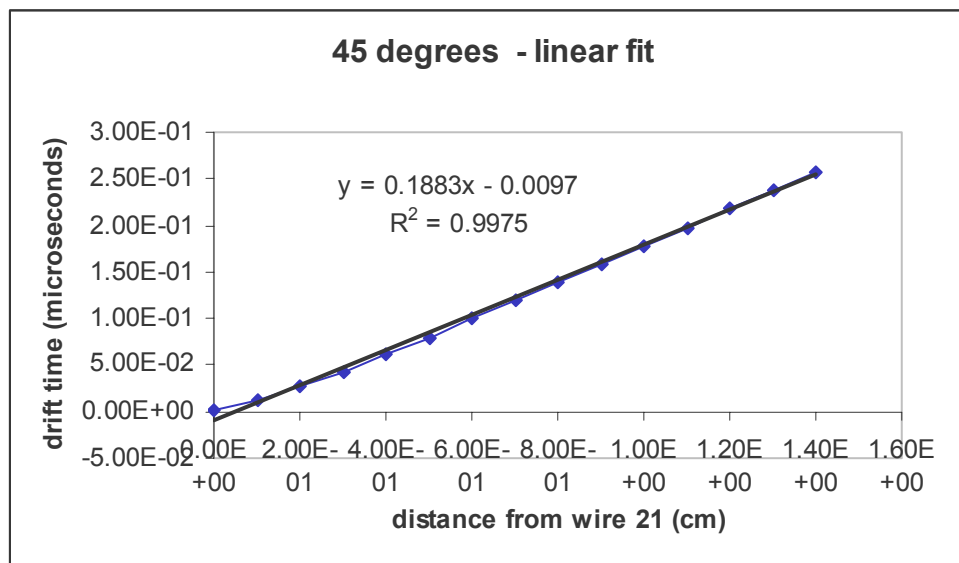
Printed at 20:34:52 on 02/04/04 with Garfield version 7.10.

Figures 5.3 (above) and 5.4 (below) represent X(t) plots directly from Garfield and MS Excel respectively.



As one can see from Table 1, the slope of the linear section is mostly invariant with the change in angle (maximum variation of 0.06 cm yields a 3% error). By contrast it is apparent that the slope of the linear fit to the entire set of data decreases as the angle increases. The reason for this is as follows. GARFIELD allows the user to define the step size along the X-axis only. For the simulation we then rotated the planes of the voltage so that the wires are defined along the Y-axis. Since the steps are still taken along the X-axis, higher angles generate more track points within the avalanche region of a particular wire. What we see from the decrease in slope is an inability of the linear fit to accurately describe the data points as a result of the increase in the effect of the avalanche region.

Visually or numerically comparing Figures 5.5 and 5.6 demonstrates the degree of error present in enforcing a linear fit on the data especially at large angles. More importantly, it illustrates the need for an equation for the drift time and track position of the particle dependent on angle  $\theta$  as well, which will be addressed in the remainder of Chapter Five. The next step would be to determine if another fit better describes the data. For this we used a quadratic fit. Table 2 lists the quadratic term of the quadratic fits for the whole set of data and the avalanche region and their respective  $R^2$  value.



Figures 5.5 (above) and 5.6 (below) compare the linear fits of the data from the smallest and largest angles simulated.

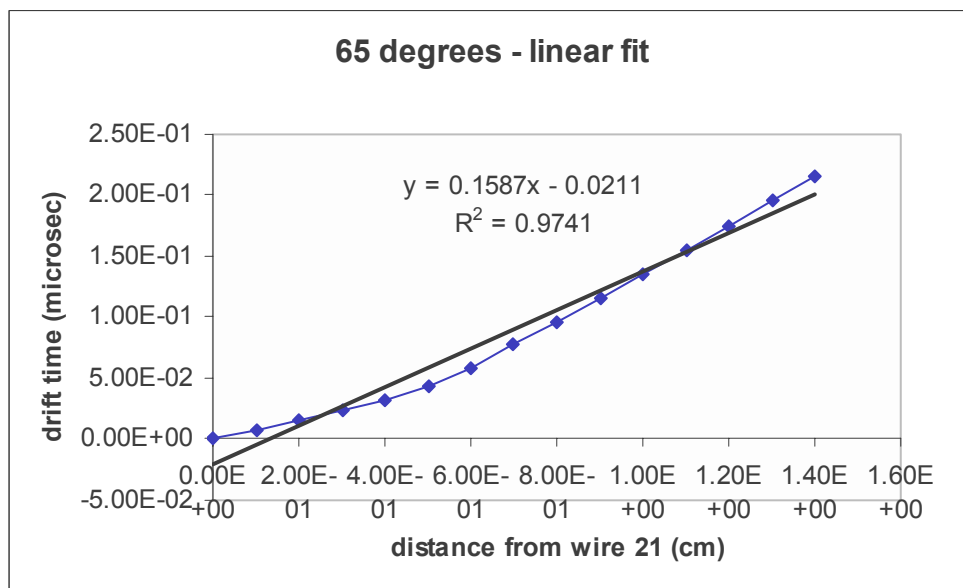
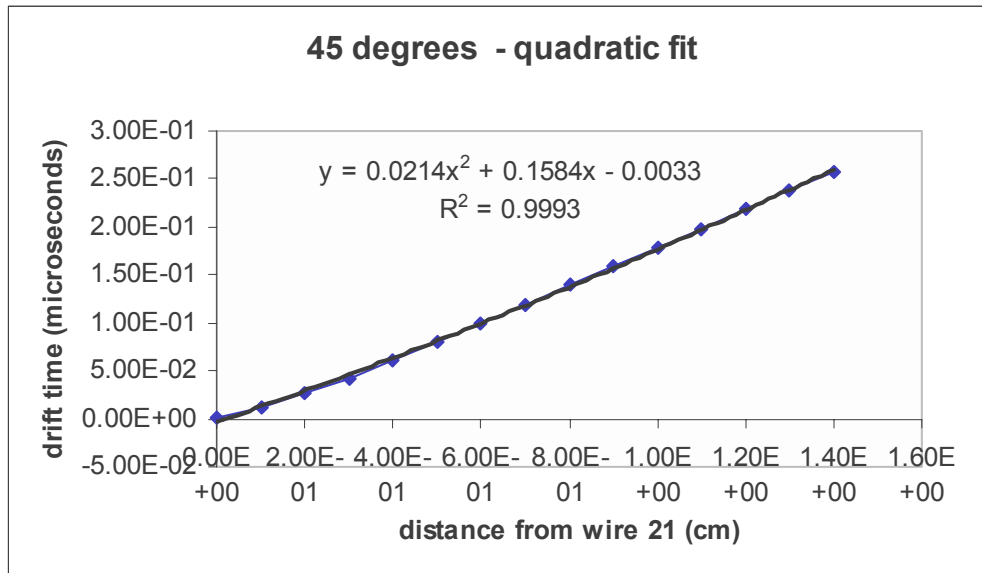


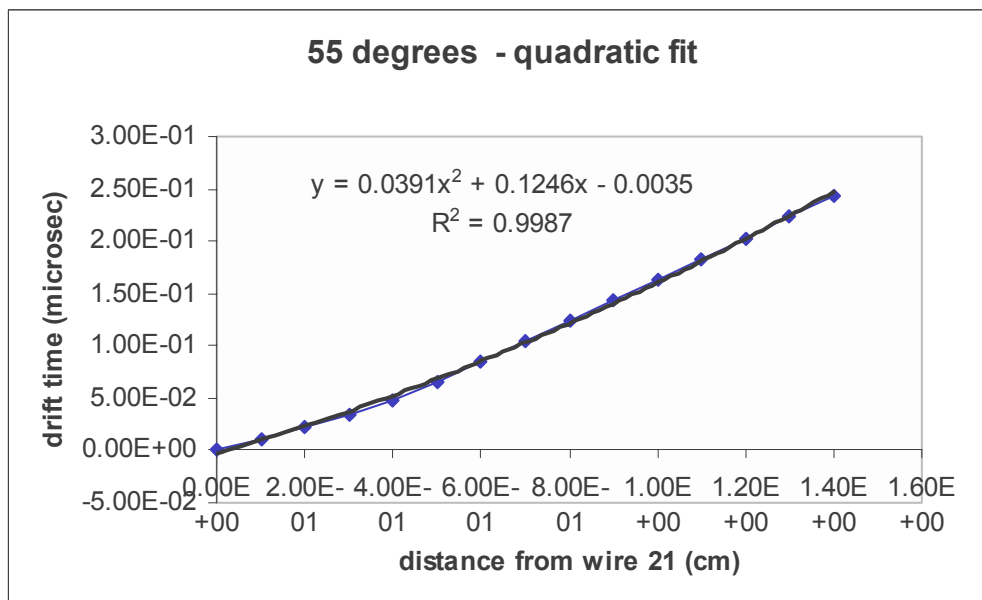
Table 2 – Slopes of quadratic equation of whole graph and Avalanche region

| $\theta$ | Full quadratic fit | $R^2$  | Avalanche section | $R^2$  |
|----------|--------------------|--------|-------------------|--------|
| 45       | 0.0214             | 0.9993 | 0.0946            | 0.9999 |
| 47       | 0.0247             | 0.9993 | 0.0945            | 0.9999 |
| 49       | 0.0279             | 0.9992 | 0.0930            | 0.9999 |
| 51       | 0.0308             | 0.9990 | 0.0912            | 0.9998 |
| 53       | 0.0347             | 0.9989 | 0.0826            | 0.9998 |
| 55       | 0.0391             | 0.9987 | 0.0785            | 0.9997 |
| 57       | 0.0427             | 0.9885 | 0.0682            | 0.9997 |
| 59       | 0.0479             | 0.9984 | 0.0549            | 0.9996 |
| 61       | 0.0532             | 0.9982 | 0.0479            | 0.9994 |
| 63       | 0.0589             | 0.9981 | 0.0369            | 0.9991 |
| 65       | 0.0647             | 0.9980 | 0.0343            | 0.9987 |

From Table 2, the slope in the avalanche region decreases with increases in angle. By contrast the slope of the overall quadratic fit increases with increase in angle. Since the drift times are smaller for larger angles, the curvature of the plot of the avalanche region is more spread out for larger angles. The increase in slope for the overall quadratic shows that since the avalanche region is spreading out in curvature, the effect is more noticeable compared with the linear section. Examining the  $R^2$  values in Table 5.2, one finds that as the angle increases, the ability of a quadratic equation to fit the entire plot decreases, although the  $R^2$  values themselves are very good. This is more easily demonstrated by a comparison of plots.



Figures 5.7 (above), 5.8(below) show the quadratic fit for the data for two angles simulated.



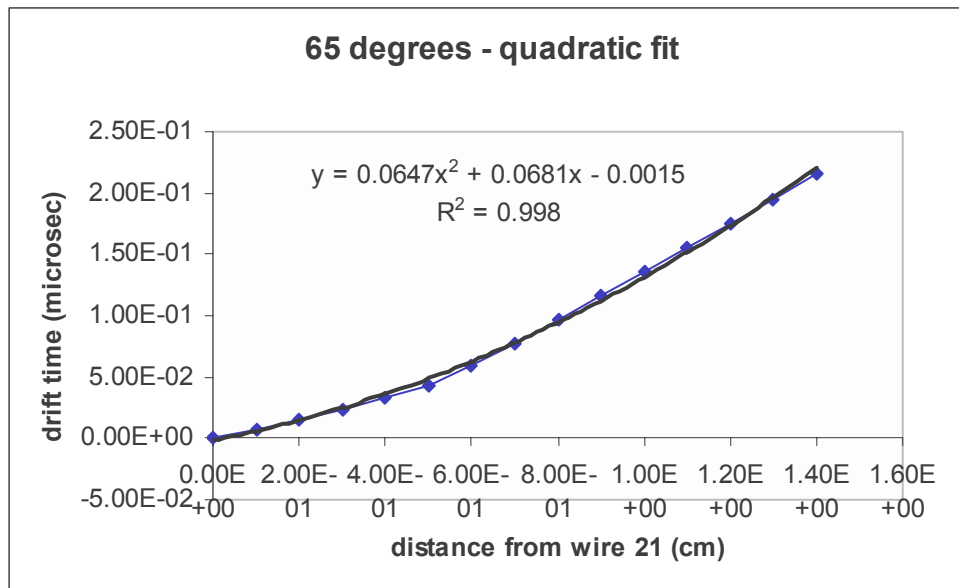


Figure 5.9 shows the quadratic fir for the largest angle simulated.

Comparing the three figures visually, one can see that the latter two plots have greater variation from the points on the plot to the fitted line. Table 3 below compares the values of X and Y from the track and from the fitted equations. Picking three points on the plot of 65 ° where the fitted plot appears to be inaccurate reveals the following:

Table 3 - Comparison of track measurements and quadratic fit

| $X_{\text{track}}$ (cm) | $Y_{\text{track}}$ ( $\mu\text{s}$ ) | $Y_{\text{fitted}}$ ( $\mu\text{s}$ ) | $\Delta t$ | X fitted (cm) | $\Delta x$ ( $\mu\text{m}$ ) |
|-------------------------|--------------------------------------|---------------------------------------|------------|---------------|------------------------------|
| 0.4                     | 0.0326                               | 0.0361                                | 0.0035     | 0.3704        | 296                          |
| 0.5                     | 0.0433                               | 0.0487                                | 0.0054     | 0.4583        | 417                          |
| 0.9                     | 0.1160                               | 0.1122                                | 0.0038     | 0.9205        | 205                          |

The table above shows the  $\Delta t$  to be on the order of 0.005  $\mu\text{s}$ . By plugging the time from the data back into the equation we find the  $\Delta x$ . The  $\Delta x$  values yield a difference of 205-417 microns between the quadratic fit and the track for 65 °, which is clearly an

unacceptable error measurement since the  $Q_{\text{weak}}$  experiment aims to have a  $200\mu\text{m}$  resolution for the chamber.

From the attempt to fit the track to a purely linear or quadratic line, we see that neither are adequate representations. However, as in Table 1, a linear fit for the region outside of the avalanche region has very little variation in slope with variation in angle. Far away from the wire, the avalanche effect is nonexistent; therefore, the drift time is dependent only on the properties of the gas and therefore should not vary with angle. Comparing the slopes of Table 1 confirms this. The expected drift velocity for the gas mixture used (ethane50-argon50) is known to be  $5\text{ cm}/\mu\text{s}$ . The inverse of the median slope value from Table 1 gives us a drift velocity of  $5.053\text{ cm}/\mu\text{s}$  for the linear region. This shows that outside of the avalanche region, the linear fit not only closely fits the data but closely matches the expected drift velocity for that gas mixture. The next logical step seems to be to find a fit for the avalanche region alone and combine that with the linear equation for the linear region to have one complete equation for each given angle.

From the lack of major variation in the fit of the linear section of the data, determining an equation for the linear section is relatively simple. Determining an equation for the avalanche region is more difficult. To increase accuracy, a second set of simulations for the avalanche region was run generating more data points to fit to a quadratic. Instead of taking 10 data points throughout the entire track with a step size of 0.05, I chose to consider only points within the avalanche region defined as under 0.4 centimeters and lowered the step size to 0.0125, increasing the number of data points to increase the accuracy of fit.

Table 4 – Coefficients for Quadratic equation of Avalanche Region

| $\theta$ | Quadratic Term | Intercept | $R^2$  |
|----------|----------------|-----------|--------|
| 45       | 0.0710         | 0.0010    | 0.9997 |
| 47       | 0.0568         | 0.0011    | 0.9997 |
| 49       | 0.0454         | 0.0012    | 0.9997 |
| 51       | 0.0365         | 0.0012    | 0.9997 |
| 53       | 0.0300         | 0.0013    | 0.9996 |
| 55       | 0.0252         | 0.0013    | 0.9996 |
| 57       | 0.0219         | 0.0013    | 0.9995 |
| 59       | 0.0203         | 0.0013    | 0.9994 |
| 61       | 0.0188         | 0.0013    | 0.9993 |
| 63       | 0.0190         | 0.0013    | 0.9992 |
| 65       | 0.0191         | 0.0013    | 0.9991 |

Comparing the quadratic terms in Table 4 we see that the quadratic decreases with increase in angle. As mentioned previously, this is a result of lower drift times for the avalanche region for higher angles. The curve of the avalanche region is more spread out. Previously it was discussed in the context of the effect of higher angles on fitting the data set to a linear fit. This means that for the avalanche region, we will need a different equation for each angle whereas for the linear region, we can use an approximate linear fit since the deviation is so low. So for each angle we have two equations, one for the linear region and one for the quadratic avalanche region (Figure 5.10). I chose to extend the linear region from 0.5 cm (Table 1) to 0.4 cm (Table 5) from the wire in order to provide a more inclusive set of data for all data points explored. Attempting to extend the avalanche region to 0.5 cm yielded a less accurate fit than the linear extended to 0.5 cm, so although the results  $\approx 0.4$  cm yield large error percentages, it seems to be the best I could do with the data provided by GARFIELD (See Appendix B for table of data points for 65°).

Table 5 – Equations for Linear and Quadratic regions

| $\theta$ | Avalanche Equation (0.00cm – 0.4cm) | Linear Equation (0.4cm – 1.4 cm) |
|----------|-------------------------------------|----------------------------------|
| 45       | $y = 0.071x^2 + 0.1301x - 0.001$    | $y = 0.1975x - 0.0189$           |
| 47       | $y = 0.0568x^2 + 0.1282x - 0.0011$  | $y = 0.1977x - 0.0215$           |
| 49       | $y = 0.0454x^2 + 0.1254x - 0.0012$  | $y = 0.1978x - 0.0241$           |
| 51       | $y = 0.0365x^2 + 0.1218x - 0.0012$  | $y = 0.1972x - 0.0266$           |
| 53       | $y = 0.03x^2 + 0.1175x - 0.0013$    | $y = 0.1969x - 0.0296$           |
| 55       | $y = 0.0252x^2 + 0.1125x - 0.0013$  | $y = 0.1968x - 0.0329$           |
| 57       | $y = 0.0219x^2 + 0.1071x - 0.0013$  | $y = 0.1956x - 0.0360$           |
| 59       | $y = 0.0203x^2 + 0.1009x - 0.0013$  | $y = 0.195x - 0.0399$            |
| 61       | $y = 0.0188x^2 + 0.0948x - 0.0013$  | $y = 0.1933x - 0.0435$           |
| 63       | $y = 0.019x^2 + 0.0878x - 0.0013$   | $y = 0.1914x - 0.0473$           |
| 65       | $y = 0.0191x^2 + 0.081x - 0.0013$   | $y = 0.188x - 0.0508$            |

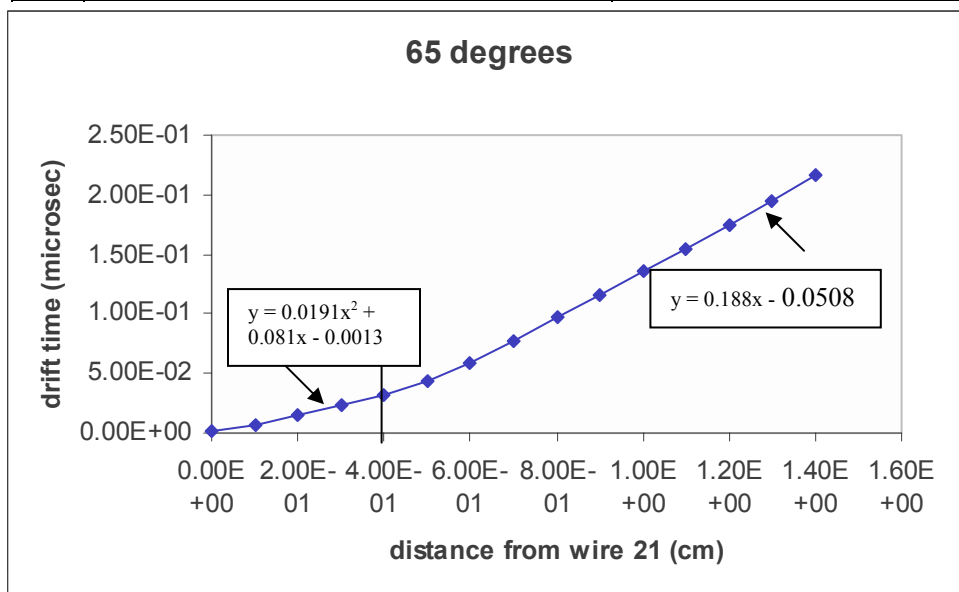


Figure 5.10 – Illustrates the demarcation between avalanche and linear regions and the relative equations for each for 65 °.

The  $X(t)$  plot for 65° is displayed in Figure 5.10 above. For  $x < 0.04$  cm, the plot follows the quadratic equation and for  $x > 0.04$  cm, the plot follows the linear equation. As noted before the linear equations vary little angle to angle, therefore it is only the quadratic of the avalanche region that varies and is necessary to determine for each angle.

The unfortunate side effect is that the graph is discontinuous at the point 0.4 cm. The limits of Microsoft Excel prevented me from fixing the linear terms constant and varying only the quadratic term, which would have allowed me to merge the two equations into a single cohesive continuous equation. The linear equation yield  $t(0.4 \text{ cm}) = 0.024 \text{ } \mu\text{s}$ , whereas the quadratic part equation yields  $t(0.4 \text{ cm}) = 0.034 \text{ } \mu\text{s}$ . Using those equations for  $65^\circ$  and plugging the  $x$  points into the equations allows one to compare the change in drift time due to the error. Similarly, plugging the known drift time (from data) into the equations gives you the estimated distance, which compared with the known track position gives the correctional constant.

Using the following equations (where  $x_{\text{perp}}$  is the true perpendicular distance and  $x_g$  is the distance measured by GARFIELD),

$$x_{\text{perp}} = v_D t_{\text{meas}} + x_{\text{corr}} \quad (6)$$

$$x_{\text{corr}} = x_g - v_D t_g \quad (7)$$

we can find  $x_{\text{corr}}$  and hence  $x_{\text{perp}}$  by inserting the data we have in Table 6 into these equations. Table 6 is a combination of the two equations given for 65 degrees. The values from  $0.0 < x < 0.4$  were from the equation for the avalanche region,  $y = 0.0191x^2 + 0.081x - 0.0013$ . The data points for  $x > 0.04$  cm are from the linear equation,  $y = 0.188x - 0.0508$  (Table 5). I included the same  $x$  value ( $x = 0.04$  cm) for both equations to give more statistics for comparing error in the line of best fit.

Table 6 – Error in line of best fit for 65°

| $X_{\text{track}}$ (cm)<br>(xg) | $Y_{\text{track}}$ ( $\mu\text{s}$ )<br>(tmeas) | $Y_{\text{fitted}}$ ( $\mu\text{s}$ )<br>(tg) | $\Delta t$ | $X_{\text{fitted}}$<br>(cm) | $\Delta x$ ( $\mu\text{m}$ ) |
|---------------------------------|---|---|------------|-----------------------------|------------------------------|
| 0.0                             | 0.0   | 0.0057  | 0.0057     | 0.01154                     | 115.4                        |
| 0.05                            | 0.00236   | 0.00311                                       | 0.00075    | 0.0407                      | 93.0                         |
| 0.1                             | 0.00672   | 0.00716                                       | 0.00044    | 0.0945                      | 55.0                         |
| 0.15                            | 0.0113  | 0.0112  | 0.0001     | 0.1511                      | 11.0                         |
| 0.2                             | 0.0159  | 0.0153  | 0.0006     | 0.2078                      | 78.0                         |
| 0.25                            | 0.0204  | 0.0193  | 0.0011     | 0.2634                      | 134                          |
| 0.3                             | 0.0249  | 0.0234  | 0.0015     | 0.3190                      | 190                          |
| 0.35                            | 0.0294  | 0.0274  | 0.0002     | 0.3745                      | 245                          |
| 0.4                             | 0.0339  | 0.0315  | 0.0024     | 0.4301                      | 301                          |
| 0.4                             | 0.0326  | 0.0244  | 0.0082     | 0.4436                      | 436                          |
| 0.5                             | 0.0433  | 0.0432  | 0.0001     | 0.5005                      | 5                            |
| 0.6                             | 0.0590  | 0.062   | 0.003      | 0.5840                      | 160                          |
| 0.7                             | 0.0771  | 0.0808  | 0.0037     | 0.6803                      | 197                          |
| 0.8                             | 0.0965  | 0.0996  | 0.0031     | 0.7835                      | 165                          |
| 0.9                             | 0.116   | 0.1184  | 0.0024     | 0.8872                      | 128                          |
| 1.0                             | 0.136   | 0.1372  | 0.0012     | 0.9936                      | 64                           |
| 1.1                             | 0.155   | 0.156   | 0.001      | 1.0947                      | 53                           |
| 1.2                             | 0.175   | 0.1748  | 0.0002     | 1.2011                      | 11                           |
| 1.3                             | 0.195   | 0.1936  | 0.0014     | 1.3074                      | 74                           |
| 1.4                             | 0.216   | 0.2124  | 0.0036     | 1.4191                      | 191                          |

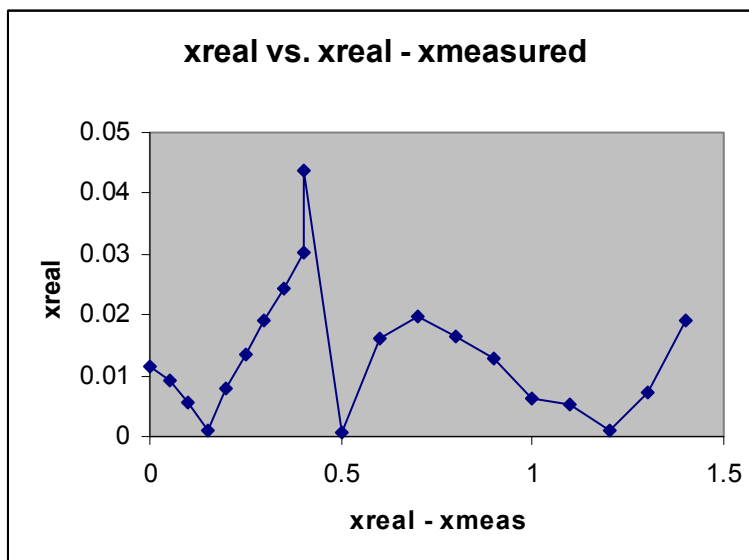


Figure 5.11 – This plot is the representation of the variation between the true vertical distance to the wire and its measurement versus the true vertical distance.

From Figure 5.11, we see that except for the one peak where the equations do not converge (around 0.4 cm from the wire), the difference between the real vertical distance and the measured distance is pretty minimal, yielding a margin of error under 200 microns at most, which is clearly within the intended margin of error ( $\approx 200 \mu\text{m}$ )

We have determined that the  $x(t)$  plot depends on the angle ( $\theta$ ) of the track. Now it is time to discuss how this information can be applied to  $Q_{\text{weak}}$ . In the actual experiment the track will be unknown. The drift time is the only information measured. From the drift time of various electrons, the track can be reconstructed, albeit with difficulty. Knowing the drift time and estimating the drift velocity (known for a given gas mixture away from avalanche region), one can guess the approximate  $x$  position. Using several guessed  $x$ -positions, one can guess the track. The method from here involves some creativity. Lining up the guessed points, one can create a line of best fit and measure an approximate angle from that. From there, one can check by plugging the known drift time into the equation for the angle immediately larger than the guessed angle in the table and compare the  $x$ -position given by the equation to the  $x$ -position approximated by the drift time. From there one can choose the angle immediately smaller than the guessed angle and repeat the process. This iteration allows one to determine the track more accurately. Neither the original guessed  $x$ -positions nor the  $x$ -positions determined by the interpolated angles will be accurate, but the accurate  $x$ -position can be found in the range of these  $x$ -positions and hence the interpolation allows one to narrow down the range of guesses for the track and more accurately determine the original track of the electron (See

Figure 3.1). Fitting simulations to linear or quadratic equations generates a lookup table that should allow for more accurate range of tracks.

## 5.4 Conclusion

The  $Q_{\text{weak}}$  experiment seeks a more precise measurement of the proton's weak charge. The Vertical Drift Chambers allow one to determine on an event-by-event basis whether an electron hitting the Cerenkov detectors is the result of an elastic or inelastic collision as well as determine its track and position on the detector. Determining this distance gives the number of hits by electrons with spin either parallel or anti-parallel to the wire and hence the asymmetry. Since the asymmetry is known (Equation 2) and the  $Q^2$  is held constant, the weak charge of the proton can be known to a certain degree of accuracy.

The simulations of drift chamber operations allow the researchers to construct the ideal drift chamber for this experiment. The simulations performed in this thesis also allow the researchers to have a basis for comparison. The tables provided in this thesis act as lookup tables for variables such as track angles. By comparing the data and equations from two track angles, one can more accurately determine  $x_{\text{perp}}$ . Using simulations from GARFIELD in conjunction with simulations through GEANT and other simulators to simulate the entire experiment, the researchers involved can gain a better understanding of what kinds of behavior to expect of the drift chambers and modify schematics if needed. With expected results from simulations to compare to experimental values at Jefferson Lab, any deviation from the Standard Model that may exist can be found. Lack of deviation would confirm the Standard Model's predictions and provide a clearer picture of the relationship between the Electromagnetic force and weak forces at small momentum transfer.

## Appendix A. Garfield Input

All Garfield input files used to create data in paper are included in this appendix and commented for ease in comprehension. Klaus Grimm or else the author of this paper created the input files used. Complete input files provided by Klaus Grimm are attributed as such. Any modifications to the input created by Dr. Grimm are mine.

### A.1 Cell

```

OPTIONS PROGRESS-PRINT

GLOBAL anode = -4100
GLOBAL wdiameter = 0.002 // 20um
GLOBAL wypos = 0.0
GLOBAL wpot = 0.0
GLOBAL wtension = 70.0 // 70g
GLOBAL wlength = 25.0*1.141 // 45grad

Global gas_file `Arg-50-Eth-50.gas`
Global gas_member `a50e50`

//=====
& CELL
//=====

opt cell-pr

plane y=-1.3 v={anode}
plane y=+1.3 v={anode}

// we use Cartesian system
ROWS CARTESIAN
  S 41 {wdiameter} -8.46+(0.423*I) ...
  {wypos} ...
  {wpot} ...
  {wtension} ...
  {wlength} ...
  TUNGSTEN

GRAVITY 0 0 1

WRITE DATASET vdc_cell.dat

```

## A.2 Gas Parameters

The & Gas section establishes the gas mixtures when drifting electrons and ions.

Garfield interfaces with programs such as the Magboltz program, which will calculate the electron drift velocity, diffusion, Townsend and attachment coefficient for various gas mixtures. Garfield also works through the Heed program to handling clustering [2].

```
//=====
& GAS
//=====

// 1 atm 50/50 Argon-ethane mixture in your chamber.

Call inquire_member(gas_file,gas_member,`gas`,exist)
If exist Then
  get {gas_file,gas_member}
Else
  write {gas_file,gas_member}

// Loads the mixture Argon 50 %, ethane 50 %
ARG-50-ETH-50

// temp + pressure def before Heed
TEMPERATURE 300 KELVIN
PRESSURE {1*1013.25} MILLI-BAR

// Compute for electrons: drift velocity, diffusion coefficient etc
// time consuming: several hours on 2.4GHz Xeon
MAGBOLTZ argon 50 ethane 50

// (Tong put it outside if-else-endif ?!)
// Prepares cluster generation by Heed
Heed argon 50 ethane 50

Endif

// Plot some gas properties
// plot-options drift-velocity nodiffusion notownsend

opt gas-plot nogas-print
```

### A.3 Electric Field

The field section allows the user to plot histograms, contour plots, vector fields and other quantities associated with an electric field.

```

OPTIONS PROGRESS-PRINT

GLOBAL anode = -4100
GLOBAL wdiameter = 0.002 // 20um
GLOBAL wypos = 0.0
GLOBAL wpot = 0.0
GLOBAL wtension = 70.0 // 70g
GLOBAL wlength = 25.0*1.141 // 45grad

Global gas_file `Arg-50-Eth-50.gas`
Global gas_member `a50e50`

//=====
& CELL
//=====

opt cell-pr

plane y=-1.3 v={anode}
plane y=+1.3 v={anode}

ROWS CARTESIAN
  S 41 {wdiameter} -8.46+(0.423*I) ...
  {wypos} ...
  {wpot} ...
  {wtension} ...
  {wlength} ...
  TUNGSTEN

GRAVITY 0 0 1

WRITE DATASET vdc_cell.dat

//=====
& MAGNETIC
//=====

// at present: no B field here
// what about the earth B field?!
COMPONENTS 0 0 0 GAUSS

//=====
& GAS
//=====

// 1 atm 50/50 Argon-ethane mixture in your chamber.

```

```

Call inquire_member(gas_file,gas_member,`gas`,exist)
If exist Then
  get {gas_file,gas_member}
Else
  write {gas_file,gas_member}

// Loads the mixture Argon 50 %, ethane 50 %
ARG-50-ETH-50

// temp + pressure def before Heed
TEMPERATURE 300 KELVIN
PRESSURE {1*1013.25} MILLI-BAR

// Compute for electrons: drift velocity, diffusion coefficient etc
// time consuming: several hours on 2.4GHz Xeon
MAGBOLTZ argon 50 ethane 50

// (Tong put it outside if-else-endif ?!)
// Prepares cluster generation by Heed
Heed argon 50 ethane 50

Endif

opt gas-plot nogas-print

//=====
& OPTIMISE
//=====

//Prints the current potential settings
DISPLAY

//forces acting on a wire and the wire displacement
SELECT 21
FORCES PRINT-SAG PLOT-SAG KEEP-SAG DETAILED ...
ELECTROSTATICS GRAVITY

//=====
& FIELD
//=====

AREA -1.5 -1.5 +1.5 +1.5

// Plot electrical field
track -1.3 0.0 -0.01 0.0
PLOT-FIELD GRAPH sqrt(EX**2+EY**2)

track * * -0.3 *
PLOT-FIELD GRAPH sqrt(EX**2+EY**2)

track -0.3 * -0.05 *
PLOT-FIELD GRAPH sqrt(EX**2+EY**2)

track -0.05 * -0.0001 *
PLOT-FIELD GRAPH sqrt(EX**2+EY**2)

```

```
// Plot contour of Electrostatic potential
grid 25
area * -.423 * .423
PLOT-FIELD CONTOUR -V RANGE 1200 4000 n=14

area -.423 * .423 *
PLOT-FIELD CONTOUR -V RANGE 900 2100 n=24
```

## A.4 Drift Properties

### A.4.1 DRIFT

Some comments included in previous sections of input have been omitted for space considerations. For the remainder of this Appendix, extraneous comments that have been previously viewed will be absent from the input files provided. Please see previous sections for comments on previously mentioned sections of Garfield input files.

```
OPTIONS PROGRESS-PRINT

GLOBAL anode = -4100
GLOBAL wdiameter = 0.002 // 20um
GLOBAL wypos = 0.0
GLOBAL wpot = 0.0
GLOBAL wtension = 70.0 // 70g
GLOBAL wlength = 25.0*1.141 // 45grad

Global gas_file `Arg-50-Eth-50.gas`
Global gas_member `a50e50`

//=====
& CELL
//=====

opt cell-pr

plane y=-1.3 v={anode}
plane y=+1.3 v={anode}

ROWS CARTESIAN
S 41 {wdiameter} -8.46+(0.423*I) ...
  {wypos} ...
  {wpot} ...
  {wtension} ...
  {wlength} ...
```

```

TUNGSTEN

GRAVITY 0 0 1

WRITE DATASET vdc_cell.dat

//=====
& MAGNETIC
//=====

COMPONENTS 0 0 0 GAUSS

//=====
& GAS
//=====

Call inquire_member(gas_file,gas_member,`gas`,exist)
If exist Then
  get {gas_file,gas_member}
Else
  write {gas_file,gas_member}

ARG-50-ETH-50

TEMPERATURE 300 KELVIN
PRESSURE {1*1013.25} MILLI-BAR

MAGBOLTZ argon 50 ethane 50
Heed argon 50 ethane 50

Endif

opt gas-plot nogas-print

//=====
& OPTIMISE
//=====

DISPLAY

//forces acting on a wire and the wire displacement
SELECT 21
FORCES PRINT-SAG PLOT-SAG KEEP-SAG DETAILED ...
ELECTROSTATICS GRAVITY

//=====
& DRIFT
//=====

//Sets the size and view of the drift area
AREA -1.5 -1.5 +1.5 +1.5

//Number of drift lines used by x(t) etc.
LINES 60

```

```

//Grid density for tables and contour plots
GRID 10 20

// define area around wire #21 for possible plots
SELECT 21                // select center wire

INTEGRATION-PARAMETERS COMPUTE-IF-INTERPOLATION-FAILS

// define single track: 45deg
TRACK  -1.5 -1.5 1.5 1.5

// Heed takes care of cluster generation, it simulates the ionization
// of the gas molecules by a particle.
TRACK HEED ...
  NODELTA-ELECTRONS NOTRACE-DELTA-ELECTRONS ...
  NOMULTIPLE-SCATTERING ...
  NOENERGY-CUT ELECTRON ENERGY 0.85 GeV

// drift line calculation:
// will begin at some of the boundaries of the drift area as set by
// AREA.
// DRIFT EDGE notleft notright up down isochrone 0.020

// drift line calculation:
// electrons or ions start to drift from the surfaces of the wires
// that have been SELECTed.
//DRIFT WIRE lines 30 isochrone 0.020

// drift line calculation: will begin on the track.
// DRIFT TRACK TIME-GRAPH CONTOUR 0.020

```

## A.4.2 X-T PLOT

The following input was used to generate the data found in the tables of drift times in Appendix B. The data from those tables was used to create table (x.x) and the X-T plots (x.x) to be compared with the X-T plots generated by Garfield which are included in Appendix C.

```

//=====
// Garfield V8.1 Input file for:
//
// Vertical Drift Chamber (VDC) Simulation
// for the Qweak experiment at JLab
//

```

```

// => Simulation of the XT-Plot
//   Correlation between perp. track distance to the wire plane and
//   the drift time of the first electron hitting the selected wire
//
//=====
// VDC Realization in Garfield:
//
// VDC consists of one wire plane and two HV planes
//
//=====
//
// Author: Klaus Grimm
//   Department of Physics
//   The College of William and Mary
//   Williamsburg, VA 23185
//
// email: grimm@jlab.org
//
// Modified by Erin Epperson 04/07/2004
//
//=====
// Last Change: 04/02/2004
//=====

GLOBAL tanglemin    = 45.0
GLOBAL tanglemax    = 65.0
GLOBAL tanglestep   = 2.0

GLOBAL xstep        = 0.05           // Stepping size in X for tracks
                                   // (0.05=500um) Changed to 0.25 and
                                   // then 0.125 for avalanche region
                                   // for more precise results

GLOBAL plane        = 1.3           // distance wire plane to HV plane
(13mm)
GLOBAL pitch        = 0.423         // perp. distance between signal
wires (4.23mm)
GLOBAL apitch       = 0.423*0.5     // half top pitch size used for
ARRIVAL-TIME-DISTRIBUTION
GLOBAL tpitch       = apitch*1.41   // bit more than bottom half pitch
size used for TIMING

Global gas_file     `Arg-50-Eth-50.gas`
Global gas_member   `a50e50`

//=====
& CELL
//=====

// Read &CELL definition
READ vdc_cell.dat

// Gravity points perp. to HV plane = x direction
GRAVITY 1 0 0

```

```

//=====
& MAGNETIC
//=====

// at present: no B field here
// what about the earth B field?!
COMPONENTS 0 0 0 GAUSS

//=====
& GAS
//=====

// 1 atm 50/50 Argon-ethane mixture in your chamber.

// Load (existing) gas_file, which contains all
// the gas properties needed for tracking
  GET {gas_file,gas_member}

// Prepares cluster generation by Heed
  Heed argon 50 ethane 50

// Plot some gas properties
// plot-options drift-velocity nodiffusion notownsend
// opt gas-plot nogas-print

//=====
& OPTIMISE
//=====

//Prints the current potential settings
DISPLAY

//forces acting on a wire and the wire displacement
SELECT 21
FORCES PRINT-SAG PLOT-SAG KEEP-SAG DETAILED ...
ELECTROSTATICS GRAVITY

//=====
& DRIFT
//=====

INTEGRATION-PARAMETERS COMPUTE-IF-INTERPOLATION-FAILS

// Heed takes care of cluster generation, it simulates the ionization
// of the gas molecules by a particle.
TRACK HEED ...
  NODELTA-ELECTRONS NOTRACE-DELTA-ELECTRONS ...
  NOMULTIPLE-SCATTERING ...
  NOENERGY-CUT ELECTRON ENERGY 0.85 GeV

//Sets the size and view of the drift area
AREA {-1.1*plane, -1.0*tpitch, +1.1*plane, +1.0*tpitch}

//Number of drift lines used by x(t) etc.
LINES 100

```

```

// define area around wire #21 for possible plots
SELECT 21          // select center wire

//-----
// Open Postscript file
//-----
!add meta type PostScript file-name "erin_xt.ps"
!open meta
!act meta

FOR tangle from {tanglemin} to {tanglemax} STEP {tanglestep} DO

// delete old entries from previous simulations
* %DELETE "XT_{angle}deg_S21.dat" .

// XT-PLOT: relation between the perp. position of a track and the
// drift time. This is a calibration curve used by the track
// reconstruction program. The X-Range was changed to (0.0, 0.45) for
// later simulations for more precise measurements for the avalanche
// region .

Say "Simulating now XT-PLOT for incident angle = {tangle}"

XT-PLOT ...
  ANGLE {tangle} ...
  X-RANGE {0.0 , 1.1*plane} X-STEP {xstep} ...
  PRECISION 1E-4 ...
  PLOT-XT-RELATION ...
  DATASET "XT_{tangle}deg_S21.dat"

ENDDO

//-----
// Close Postscript file
//-----
!deact meta
!close meta
!del meta

```

### A.4.3 ARRIVAL

The differences between X\_T plot and ARRIVAL-TIME-DISTRIBUTION are best illustrated in a table provided by the Garfield source data [2]:

| Aspect   | ARRIVAL  | XT-PLOT  |
|----------|--|--|
| input    | complete gas tables,<br>clustering properties<br>(spacing, cluster size)             | drift velocity and optionally<br>diffusion and Lorentz angle<br>tables                     |
| method   | Monte Carlo generation of<br>tracks with clusters                                    | parabolic minimisation of the<br>drift time over lines                                     |
| included | drift velocity, Lorentz<br>angle, diffusion, attachment,<br>cluster spacing and size | drift velocity, Lorentz angle,<br>optionally also diffusion<br>over the fastest drift line |
| output   | mean, median and RMS of<br>selected electrons  | minimum drift time, diffusion<br>over the fastest drift line                               |

The X-T PLOT function was used for the majority of data included in this paper. The reason for this is the ARRIVAL-TIME-DISTRIBUTION function took multiple days to compute data for the range of angles explored in the simulations. The X-T PLOT by comparison took a few minutes. The ARRIVAL-TIME-DISTRIBUTION data is more accurate as it includes the specifics of the gas tables and performs more physics.

```
//=====
// Garfield V8.1 Input file for:
//
//   Vertical Drift Chamber (VDC) Simulation
//   for the Qweak experiment at JLab
//
// => Simulation of the ARRIVAL-TIME-DISTRIBUTION for the n-th
//   drift electron for a given track (using)
//
//=====
// Simplified VDC layout for Garfield
//
// VDC consists of one wire plane and two HV planes.
// Garfield forces us to use this orientation of the VDC since
// in Garfield you can only define a X-RANGE **only** for a XT-PLOT ...
// (There is no YT-PLOT defined in Garfield)
//
//   |       | /
```

```

//      | * | /
//      |   |   |
//      | * / |   |   Y |
//      | / |   |   |   |
//      | * |   |   |   |
//      | / |   |   |   |
//      | / * |   |   |
//      | / | * |   |   |
//      | / | * |   |   |
//      | / | * |   |   |
//
//=====
//
// Author: Klaus Grimm
//         Department of Physics
//         The College of William and Mary
//         Williamsburg, VA 23185
//
// email: grimm@jlab.org
//
// Modified by Erin Epperson 04/07/2004
//
//=====
// Last Change: 04/02/2004
//=====

GLOBAL aiter      = 1000          // Number of tracks for ARRIVAL-TIME-
DISTRIBUTION

GLOBAL tanglemin  = 45.0
GLOBAL tanglemax  = 65.0
GLOBAL tanglestep = 2.0

GLOBAL tofmin     = 0.0          // Minimal Time of Flight for
histograms [us]
GLOBAL tofmax     = 0.3          // Minimal Time of Flight for
histograms : 300ns

GLOBAL plane      = 1.3          // distance wire plane to HV plane
(13mm)
GLOBAL pitch      = 0.423        // perp. distance between signal
wires (4.23mm)
GLOBAL apitch     = 0.423*0.5    // half top pitch size used for
ARRIVAL-TIME-DISTRIBUTION
GLOBAL tpitch     = apitch*1.41  // bit more than bottom half pitch
size used for TIMING

Global gas_file   `Arg-50-Eth-50.gas`
Global gas_member `a50e50`

//=====
& CELL
//=====

WRITE DATASET vdc_cell.dat
GRAVITY 1 0 0

```

```

//=====
& MAGNETIC
//=====

COMPONENTS 0 0 0 GAUSS

//=====
& GAS
//=====

GET {gas_file,gas_member}

HEED argon 50 ethane 50

//=====
& OPTIMISE
//=====

//Prints the current potential settings
DISPLAY

//forces acting on a wire and the wire displacement
SELECT 21
FORCES PRINT-SAG PLOT-SAG KEEP-SAG DETAILED ...
ELECTROSTATICS GRAVITY

//=====
& DRIFT
//=====

INTEGRATION-PARAMETERS COMPUTE-IF-INTERPOLATION-FAILS

// Heed takes care of cluster generation, it simulates the ionization
// of the gas molecules by a particle.
TRACK HEED ...
  NODELTA-ELECTRONS NOTRACE-DELTA-ELECTRONS ...
  NOMULTIPLE-SCATTERING ...
  NOENERGY-CUT ELECTRON ENERGY 0.85 GeV

//Sets the size and view of the drift area
AREA {-1.1*plane, -3.0*pitch, +1.1*plane, +3.0*pitch}

//Number of drift lines used by x(t) etc.
LINES 60

// define area around wire #21 for possible plots
SELECT 21 // select center wire

//-----
// Open Postscript file
//-----
!add meta type PostScript file-name "erin_arrival.ps"
!open meta
!act meta

```

```

FOR tangle from {tanglemin} to {tanglemax} STEP {tanglestep} DO

// delete old entries from previous simulations
* %DELETE "ARRIVAL_{angle}deg_S21.dat" .

//ARRIVAL-TIME-DISTRIBUTION:
//Computes the arrival time distribution of the n'th electron that
// reach electrodes from a series of tracks.
// A by-product of this calculation is the x(t) relation and an
// estimate of the arrival time spread. See XT-PLOT for a comparison
// with related commands.

Say "Simulating now ARRIVAL-TIME-DISTRIBUTION for angle = {tangle}"

ARRIVAL-TIME-DISTRIBUTION ELECTRON 1 ...
  TIME-WINDOW {tofmin , tofmax} ...
  STEP X RANGE {0.0 , 1.1*plane} INCREMENT 0.1 ...
  SCAN Y RANGE {-apitch , +apitch} ...
  ANGLE {tangle} ...
  DIFFUSION ...
  DATASET "ARRIVAL_{tangle}deg_S21.dat" ...
  ITERATIONS {aiter} ...
  PLOT-SELECTED-ELECTRONS

ENDDO

//-----
// Close Postscript file
//-----
!deact meta
!close meta
!del meta

```

#### A.4.4 SIGNAL

SIGNAL computes the signals on the electrodes in the chamber that result from the passage of a charged particle. [2]

```

//=====
// Garfield V8.1 Input file for:
//
// Vertical Drift Chamber (VDC) Simulation
// for the Qweak experiment at JLab
//
// => Simulation of a wire signal given by SIGNAL
//
//=====

```

```

// Simplified VDC layout for Garfield
//
// VDC consists of one wire plane and two HV planes.
// Garfield forces us to use this orientation of the VDC since
// in Garfield you can only define a X-RANGE **only** for a XT-PLOT ...
// (There is no YT-PLOT defined in Garfield)
//
//      |      | /
//      | *    | /
//      |      |      |
//      | *    |      |      |
//      | /    |      |      |      |
//      | *    |      |      |      |
//      | /    |      |      |      |
//      | *    |      |      |      |
//      | /    |      |      |      |
//      | *    |      |      |      |
//      | /    |      |      |      |
//      | *    |      |      |      |
//      | /    |      |      |      |
//      | *    |      |      |      |
//
//=====
//
// Author: Klaus Grimm
//         Department of Physics
//         The College of William and Mary
//         Williamsburg, VA 23185
//
// email: grimm@jlab.org
//
// Modified by Erin Epperson 04/07/2004
//
//=====
// Last Change: 05/02/2004
//=====

GLOBAL tofmin      = 0.0           // Minimal Time of Flight for
histograms [us]
GLOBAL tofmax      = 0.3           // Minimal Time of Flight for
histograms : 300ns

GLOBAL plane       = 1.3           // distance wire plane to HV plane
(13mm)
GLOBAL pitch       = 0.423         // perp. distance between signal
wires (4.23mm)
GLOBAL apitch      = 0.423*0.5     // half top pitch size used for
ARRIVAL-TIME-DISTRIBUTION
GLOBAL tpitch      = apitch*1.41   // bit more than bottom half pitch
size used for TIMING

GLOBAL anglemean   = 54.7          // mean garfield tracking angle =
54.7deg
GLOBAL anglemin    = 53.787        // min garfield tracking angle =
53.787deg
GLOBAL anglemax    = 55.673        // max garfield tracking angle =
55.673deg

Global gas_file    `Arg-50-Eth-50.gas`

```

```

Global gas_member `a50e50`

//=====
& CELL
//=====

GET vdc_cell.dat

//=====
& MAGNETIC
//=====

COMPONENTS 0 0 0 GAUSS

//=====
& GAS
//=====

// 1 atm 50/50 Argon-ethane mixture in your chamber.

// Load existing gas_file, which contains all
// the gas properties needed for tracking
  GET {gas_file,gas_member}

// Prepares cluster generation by Heed
  HEED argon 50 ethane 50

//=====
& DRIFT
//=====

INTEGRATION-PARAMETERS COMPUTE-IF-INTERPOLATION-FAILS

//-----
// Open Postscript file
//-----
!add meta type PostScript file-name "erin_signal.ps"
!open meta
!act meta

//=====
& SIGNAL
//=====

// Before issuing a SIGNAL instruction, one has to
//
// * set the time WINDOW over which signals are to be computed;
// * SELECT the electrodes to be read out.
// * set both the geometrical parameters and the clustering model of
//   the TRACK;
// * set the AVALANCHE model;

//Sets the size and view of the drift area

```

```

AREA {-1.1*plane, -1.0*tpitch, +1.1*plane, +1.0*tpitch}

// define area around wire #21 for possible plots
SELECT 21 // select center wire

// Heed takes care of cluster generation, it simulates the ionization
// of the gas molecules by a particle.
TRACK HEED ...
  NODELTA-ELECTRONS NOTRACE-DELTA-ELECTRONS ...
  NOMULTIPLE-SCATTERING ...
  NOENERGY-CUT ELECTRON ENERGY 0.85 GeV

// First define a track
TRACK {-1.1*plane, -1.1*plane, +1.1*plane, +1.1*plane}

// AVALANCHE:
// Chooses the probability distribution to be used for the avalanche
// multiplication factor, i.e. the number of electrons produced in the
// avalanche + the electron that started the avalanche. Electrons that
// are lost in attachment processes before reaching an electrode
// are included in the count. A multiplication factor of 1 means that
// there is no multiplication, factors smaller than 1 do not occur.
//
// No default type of avalanche is set !!!
// you must issue an AVALANCHE command prior to any signal calculation
//
AVALANCHE ...
  TOWNSEND

//Setting the time WINDOW over which signals are to be computed: \
// WINDOW t_start t_step [n_step]
//By default, signals start at t=0 and are sampled every 0.01 microsec.
//The number of samples is by default MXLIST, usually 200 or 1000
// depending on the compilation flags that were selected.
//
WINDOW 0.0 0.01 200

SIGNAL ...
  AVALANCHE ...
  SAMPLE-SIGNAL ...
  DIFFUSION ...
  ELECTRON-PULSE ...
  NOION-PULSE ...
  MONTE-CARLO-DRIFT-LINES ...
  NEW ...
  NOCROSS-INDUCED ...
  NOINTERPOLATE-TRACK

// Plots the signals
PLOT-SIGNALS ...
  TIME-WINDOW 0.0 0.3 ...
  RANGE AUTOMATIC ...
  WIRES S21 ...

```

```
NOCROSS-INDUCED-SIGNALS ...
DIRECT-SIGNALS
```

```
//-----
// Close Postscript file
//-----
!deact meta
!close meta
!del meta
```

## A.4.5 TIMING

```
//=====
// Garfield V8.1 Input file for:
//
// Vertical Drift Chamber (VDC) Simulation
// for the Qweak experiment at JLab
//
// => Time of Flight (TOF) spectrum given by TIMING
//
// Author: Klaus Grimm
//         Department of Physics
//         The College of William and Mary
//         Williamsburg, VA 23185
//
// email: grimm@jlab.org
//
// Modified by Erin Epperson 04/07/2004
//
//=====
// Last Change: 05/02/2004
//=====

GLOBAL titer      = 40000          // Number of tracks for TIMING

GLOBAL tofmin     = 0.0           // Minimal Time of Flight for
histograms [us]

GLOBAL tofmax     = 0.3           // Minimal Time of Flight for
histograms : 300ns

GLOBAL plane      = 1.3           // distance wire plane to HV plane
(13mm)
GLOBAL pitch      = 0.423         // perp. distance between signal
wires (4.23mm)
GLOBAL apitch     = 0.423*0.5     // half top pitch size used for
ARRIVAL-TIME-DISTRIBUTION
GLOBAL tpitch     = apitch*1.41   // bit more than bottom half pitch
size used for TIMING

GLOBAL anglemean  = 54.7          // mean garfield tracking angle =
54.7deg
GLOBAL anglemin   = 53.787       // min garfield tracking angle =
53.787deg
GLOBAL anglemax   = 55.673       // max garfield tracking angle =
```

```

55.673deg

Global gas_file      `Arg-50-Eth-50.gas`
Global gas_member    `a50e50`

//=====
& CELL
//=====

// Load &CELL definition
GET vdc_cell.dat

//=====
& MAGNETIC
//=====

COMPONENTS 0 0 0 GAUSS

//=====
& GAS
//=====

// 1 atm 50/50 Argon-ethane mixture in your chamber.

// Load existing gas_file, which contains all
// the gas properties needed for tracking
  GET {gas_file,gas_member}

// Prepares cluster generation by Heed
  HEED argon 50 ethane 50

//=====
& OPTIMISE
//=====

//Prints the current potential settings
DISPLAY

//forces acting on a wire and the wire displacement
SELECT 21
FORCES PRINT-SAG PLOT-SAG KEEP-SAG DETAILED ...
ELECTROSTATICS GRAVITY

//=====
& DRIFT
//=====

INTEGRATION-PARAMETERS COMPUTE-IF-INTERPOLATION-FAILS

// Heed takes care of cluster generation, it simulates the ionisation of
// the gas molecules by a particle.
TRACK HEED ...
  NODELTA-ELECTRONS NOTRACE-DELTA-ELECTRONS ...
  NOMULTIPLE-SCATTERING ...
  NOENERGY-CUT ELECTRON ENERGY 0.85 GeV

```

```

//Sets the size and view of the drift area
AREA {-1.1*plane, -1.0*tpitch, +1.1*plane, +1.0*tpitch}

//Number of drift lines used by XT-PLOT and TIMING.
LINES 200

// define area around wire #21 for possible plots
SELECT 21 // select center wire

//-----
// Open Postscript file
//-----
!add meta type PostScript file-name "erin_timing.ps"
!open meta
!act meta

// Last but not least (in cpu time consuming =8-)

// TIMING: Computes the arrival time distribution of the n'th electron
// over a given area. Unlike the ARRIVAL-TIME-DISTRIBUTION instruction,
// TIMING does not produce calibration curves, but merely timing
// distributions.
// -> good for (white noise) TOF spectrum

Say "Simulating now TOF Spectrum with TIMING"

TIMING ELECTRON 1 ...
  TIME-WINDOW {tofmin , tofmax} ...
  X-RANGE {-1.1*plane, 0.0} ...
  Y-RANGE {-tpitch , +tpitch} ...
  ANGLE-RANGE {anglemin , anglemax} ...
  BINS 301 ...
  ITERATIONS {titer} ...
  RUNGE-KUTTA-DRIFT ...
  PLOT-SELECTED-ELECTRON

//-----
// Close Postscript file
//-----
!deact meta
!close meta
!del meta

```

## Appendix B

This Appendix includes graphs and tables not given in the thesis which may serve to aid those seeking to understand my methods for choosing equations and cutoff points for regions.

Table 7: 65° – table of data points extracted from X(T) plot function of GARFIELD. Input given in section A.4.2

| <b>X position (distance from wire 22 out of 41 in cm)</b> | <b>Drift time (<math>\mu\text{s}</math>)</b> |
|---|--|
| 0.00E+00  | 1.23E-03                                     |
| 1.00E-01  | 7.16E-03                                     |
| 2.00E-01  | 1.58E-02                                     |
| 3.00E-01  | 2.41E-02                                     |
| 4.00E-01  | 3.26E-02                                     |
| 5.00E-01  | 4.33E-02                                     |
| 6.00E-01  | 5.90E-02                                     |
| 7.00E-01  | 7.71E-02                                     |
| 8.00E-01  | 9.65E-02                                     |
| 9.00E-01  | 1.16E-01                                     |
| 1.00E+00  | 1.36E-01                                     |
| 1.10E+00  | 1.55E-01                                     |
| 1.20E+00  | 1.75E-01                                     |
| 1.30E+00  | 1.95E-01                                     |
| 1.40E+00  | 2.16E-01                                     |

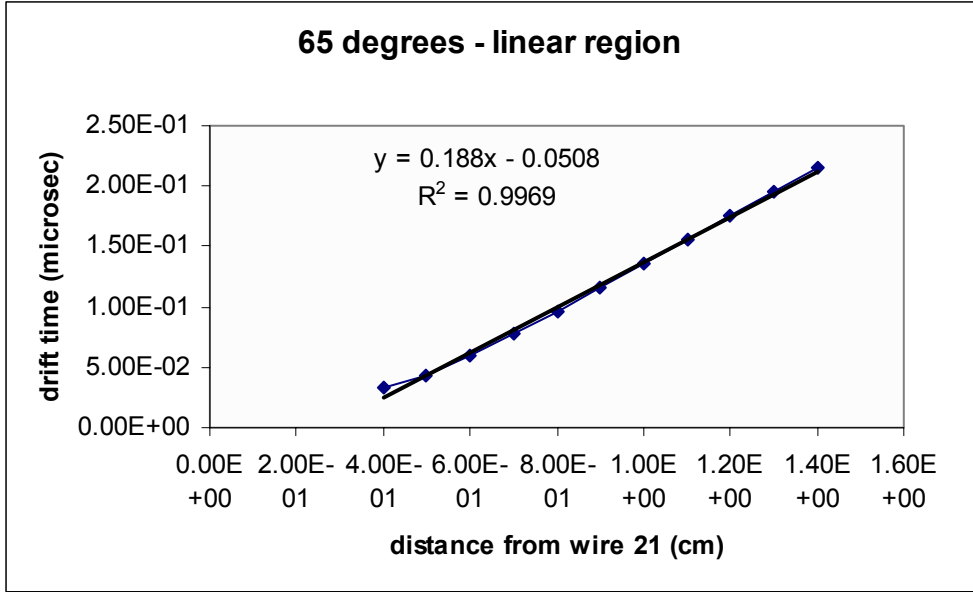


Figure B.1 - This figure is the graphical representation of the data from the linear region from Table 7.

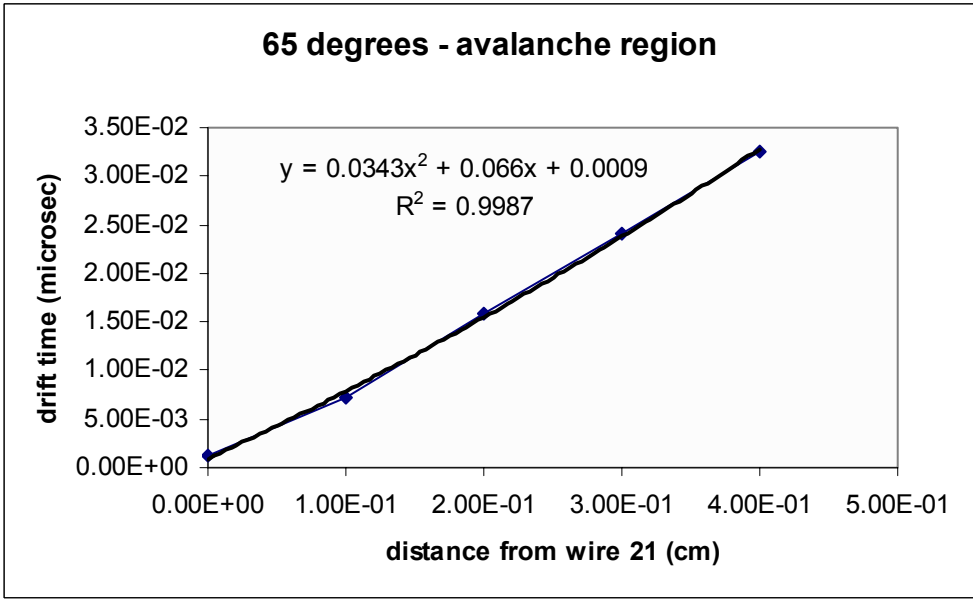


Figure B.2 - This figure is the graphical representation of the data from the avalanche region taken from Table 7.

Table 8: Second set of X(t) plot runs for 65° - Increased number of data points for within the avalanche region only. GARFIELD input given in comments in section A.4.2

| <b>X position (distance from wire in cm)</b> | <b>Drift time (<math>\mu\text{s}</math>)</b> |
|--|--|
| 0.00E+00                                     | 0.00E+00                                     |
| 1.25E-02                                     | 2.11E-04                                     |
| 2.50E-02                                     | 6.80E-04                                     |
| 3.75E-02                                     | 1.42E-03                                     |
| 5.00E-02                                     | 2.36E-03                                     |
| 6.25E-02                                     | 3.39E-03                                     |
| 7.50E-02                                     | 4.48E-03                                     |
| 8.75E-02                                     | 5.59E-03                                     |
| 1.00E-01                                     | 6.72E-03                                     |
| 1.13E-01                                     | 7.86E-03                                     |
| 1.25E-01                                     | 8.99E-03                                     |
| 1.38E-01                                     | 1.01E-02                                     |
| 1.50E-01                                     | 1.13E-02                                     |
| 1.63E-01                                     | 1.24E-02                                     |
| 1.75E-01                                     | 1.36E-02                                     |
| 1.88E-01                                     | 1.47E-02                                     |
| 2.00E-01                                     | 1.59E-02                                     |
| 2.13E-01                                     | 1.70E-02                                     |
| 2.25E-01                                     | 1.81E-02                                     |
| 2.38E-01                                     | 1.92E-02                                     |
| 2.50E-01                                     | 2.04E-02                                     |
| 2.63E-01                                     | 2.15E-02                                     |
| 2.75E-01                                     | 2.26E-02                                     |
| 2.87E-01                                     | 2.38E-02                                     |
| 3.00E-01                                     | 2.49E-02                                     |
| 3.13E-01                                     | 2.60E-02                                     |
| 3.25E-01                                     | 2.72E-02                                     |
| 3.38E-01                                     | 2.83E-02                                     |
| 3.50E-01                                     | 2.94E-02                                     |
| 3.63E-01                                     | 3.05E-02                                     |
| 3.75E-01                                     | 3.17E-02                                     |
| 3.88E-01                                     | 3.28E-02                                     |
| 4.00E-01                                     | 3.39E-02                                     |
| 4.12E-01                                     | 3.50E-02                                     |
| 4.25E-01                                     | 3.61E-02                                     |
| 4.38E-01                                     | 3.73E-02                                     |

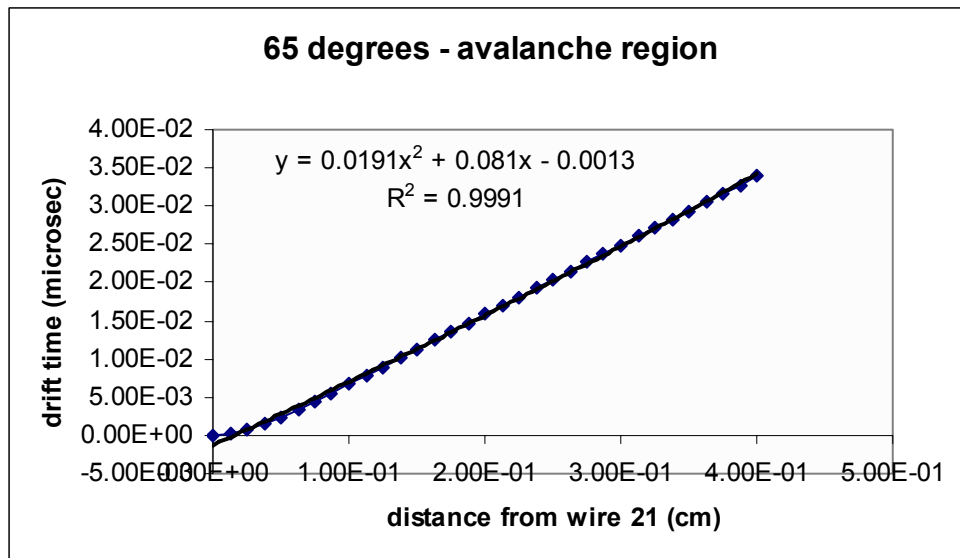


Figure B.3 - This figure is created by data from the second set of X(t) Plot generations (Table 8) which increased the number of data points in the avalanche region. I used this equation for Tables 5 and 6 in the main body of this thesis.

## References

- [1] Veenhof, Rob. “Simulation of Gaseous Detectors”. Abstract.  
<http://consult.cern.ch/writeup/garfield/>. Version 7.04. 25 Jan 2001.
- [2] Compilation and source help by Klaus Grimm  
[http://www.jlab.org/~grimm/Qweak/Garfield/Garfield\\_Sources.html](http://www.jlab.org/~grimm/Qweak/Garfield/Garfield_Sources.html)
- [3] Armstrong, et al. The  $Q_{\text{weak}}^{\text{P}}$  Experiment: “A Search for New Physics at the TeV Scale via a Measurement of the Proton’s Weak Charge” Technical Design Report. January 15, 2003.
- [4] Armstrong et al. “The  $Q_{\text{weak}}$  Experiment: A Search for New Physics at the TeV Scale Via the Measurement of the Proton’s Weak Charge.”  
“<http://www.jlab.org/qweak/>” (2001).
- [5] Sauli, F. *Principles of Multiwire Proportional and Drift Chambers*. European Organization for Nuclear Research [CERN]. Lecture. Geneva 1977.
- [6] Wechsler, Risa H. *Drift-Time Properties of CEBAF Hall A Vertical Drift Chambers* [thesis]. Cambridge (MA): Massachusetts Institute of Technology; 1996 June.
- [7] PowerPoint presentation on VDCs by Dr. Klaus Grimm in Boston  
<http://www.jlab.org/~grimm/Qweak/talks/Boston/>
- [8] Fissum, K.G., et al. “Vertical drift chambers for the Hall A high-resolution spectrometers at Jefferson Lab.” Abstract. *Nuclear Instruments and Methods in Physics Research A* 474 (2001) 108-131.
- [9] Veenhof, Rob. “Garfield, a drift-chamber simulation program User’s guide”  
Version 5.27. 6 June 1996.
- [10] Veenhof, Rob . “Garfield Help Pages”  
<http://consult.cern.ch/writeup/garfield/help/> 25 Jan 2001.